environmental microbiology

Environmental Microbiology (2021) **00**(00), 00–00 doi:10.1111/1462-2920.15485

Special Issue Article

Subzero, saline incubations of *Colwellia psychrerythraea* reveal strategies and biomarkers for sustained life in extreme icy environments

Miranda C. Mudge,[1,2] **Brook L. Nunn**,[1,3*] **Erin Firth**,[4] **Marcela Ewert**,[4] **Kianna Hales**,[1] **William E. Fondrie**,[1] **William S. Noble**,[1,5] **Jonathan Toner**,[6] **Bonnie Light**[4] **and Karen A. Junge**[4]

[1]*Department of Genome Sciences, University of Washington, Seattle, WA.*

[2]*Department of Molecular and Cellular Biology, University of Washington, Seattle, WA.*

[3]*Astrobiology Program, University of Washington, Seattle, WA.*

[4]*Applied Physics Lab, Polar Science Center, University of Washington, Seattle, WA.*

[5]*Paul G. Allen School of Computer Science and Engineering, University of Washington, Seattle, WA.*

[6]*Department of Earth and Space Sciences, University of Washington, Seattle, WA.*

Summary

Colwellia psychrerythraea **is a marine psychrophilic bacterium known for its remarkable ability to maintain activity during long-term exposure to extreme subzero temperatures and correspondingly high salinities in sea ice. These microorganisms must have adaptations to both high salinity and low temperature to survive, be metabolically active, or grow in the ice. Here, we report on an experimental design that allowed us to monitor culturability, cell abundance, activity and proteomic signatures of** ***C. psychrerythraea*** **strain 34H (*Cp*34H) in subzero brines and supercooled sea water through long-term incubations under eight conditions with varying subzero temperatures, salinities and nutrient additions. Shotgun proteomics found novel metabolic strategies used to maintain culturability in response to each independent experimental variable, particularly in pathways regulating carbon, nitrogen and fatty acid metabolism. Statistical analysis of abundances of proteins uniquely identified in isolated conditions provide metabolism-specific protein biosignatures indicative of growth or survival in either increased salinity, decreased temperature, or nutrient limitation. Additionally, to aid in the search for extant life on other icy worlds, analysis of detected short peptides in −10°C incubations after 4 months identified over 500 potential biosignatures that could indicate the presence of terrestrial-like cold-active or halophilic metabolisms on other icy worlds.**

Introduction

As seawater freezes, organisms are trapped within brine channels and inclusions. This habitable, liquid fraction of the sea ice environment is spatially heterogeneous and variably interconnected (Golden *et al*., 2007; Ewert and Deming, 2014), with decreasing temperatures resulting in reduced brine volume and increased brine salinity (Cox and Weeks, 1983). This environment is dynamic and heterogeneous over spatial and temporal scales, including many factors such as bacterial abundances and diversities, extracellular polymeric substances (EPS; Collins *et al*., 2008; Ewert *et al*., 2013) and dissolved organic carbon (Underwood *et al*., 2010). In the Arctic, conditions can be simultaneously dynamic and extreme for considerable periods of time; data recorded within sea ice near Utqiaġvik, Alaska show temperatures remaining below −10°C and calculated brine salinities remaining above 144 ppt (14.4% salt content) for greater than 100 consecutive days (Ewert and Deming, 2014). Organisms living in sea ice thus may be considered polyextremophiles, experiencing both subzero temperatures (psychrotolerance or psychrophily; Junge *et al*., 2019) and high salinities (halotolerance or halophily; Oren, 2006), as well as highly variable nutrient availability.

Polyextremophiles have a particular relevance to astrobiology, and given that most planets and moons with the

Received 13 November, 2020; accepted 22 March, 2021. *For correspondence. E-mail brookh@uw.edu; Tel. 206-616-9023; Fax 206-685-7301.

potential to harbour life have surface temperatures well below freezing with putative high salt content liquids (Hand *et al*., 2009; Martin and McMinn, 2018), it is reasonable to examine polyextremophilic psychrophiles. Of distinct interest in the search for signs of extraterrestrial life is the Europan chaos terrain (Hand *et al*., 2017, Europa Lander Report). Organisms sampled from this environment would be expected to have passed through habitable subsurface liquid into uninhabitable surface ice, thus it is important to understand the survivability of organisms and biosignatures when transferred to conditions beyond their known growth limits for considerable periods of time, specifically conditions that are colder, more saline and potentially nutrient limited. Additionally, liquid water, ranging in size from droplets to predicted subsurface oceans, has been detected on various icy worlds throughout the Solar System due to the high concentration of salts within (Carr *et al*., 1998; Hendrix *et al*., 2018; Lauro *et al*., 2020), making brines on such worlds a suitable target for the search for biomarkers of life. Martin and colleagues (2019) modelled one such example, Titan's subsurface ocean, to report potential protein compactness, flexibility and backbone dihedral distributions by comparing proteins found on Earth to simulations in Titan waters, adding weight to our hypothesis described herein that proteins can exist in extreme hypersaline conditions.

The theoretical minimum growth temperatures for psychrophilic organisms (such as those predicted for Antarctic isolates in Bowman *et al*., 1998) will be limited by the equilibrium salinity of the brines, unless the organism is inhabiting supercooled solutions. On Earth, supercooled water exists in clouds, in the surface waters of open leads or ice islands in the Arctic ocean (Untersteiner and Sommerfeld, 1964; Katsaros, 1973), or brines underneath Antarctic ice sealed lakes (Murray *et al*., 2012); evidence of bacterial activity has been observed in supercooled cloud droplets and Antarctic brines, suggesting such liquids provide suitable habitats for life (Sattler *et al*., 2001; Kuan *et al.,* 2003; Murray *et al*., 2012; Creamean *et al*., 2019). Adaptations that limit sea ice freezing, favour supercooling, or allow the organism to locate itself in conditions of favourable salinity will be advantageous to microorganisms in sea ice. Survival at subzero temperatures in equilibrium brines in comparison to supercooled seawater at the same temperature has not been examined to date. It is furthermore unclear whether low-temperature or high-salinity adaptations, or what combination of both, grant an organism the ability to grow under the corresponding equilibrium brine salinity conditions in subzero environments. Thus, in order to characterize the responses of organisms to polyextremophilic environments, we used multivariable laboratory experiments with both supercooled seawater and equilibrium brines that allowed us to investigate the individual and interactive effects of salinity and temperature and at the same time explore microbial activities in supercooled seawater.

Here, we specifically examined *Colwellia psychrerythraea* 34H (*Cp*34H), a marine psychrophilic gammaproteobacterium from subzero Arctic marine sediments (Huston *et al*., 2000) that is also found in sea ice (Methé *et al*., 2005; Boetius *et al*., 2015). *Cp*34H is considered the model marine psychrophile for cold oceans (Czajkaa *et al*., 2018); it has been shown to exhibit protein synthesis at very low subzero temperatures in artificial sea ice (Junge *et al*., 2006) and to possess many adaptations typical of psychrophilic sea ice bacteria (Methé *et al*., 2005; Ewert and Deming, 2011; Collins and Deming, 2013; Nunn *et al*., 2015; Firth *et al*., 2016; Showalter and Deming, 2018). The current temperature growth range of *Cp*34H in nutrient rich marine media is −12 to 19°C (Wells and Deming, 2006a, 2006b), corresponding to an equilibrium brine salinity maximum of approximately 181 ppt (Cox and Weeks, 1986; Eicken and Salganek, 2009), well outside the observed salinity growth range of *Cp*34H at its optimal growth temperature of 8°C in nutrient rich marine medium (15–70 ppt; Huston, 2004). The equilibrium brine conditions studied here were chosen based on natural conditions encountered by organisms within sea ice based on known eutectic point values. Below −5°C, conductive fluid flow in sea ice ceases to exist (Golden *et al*., 2007) and brine pockets containing a high salt content are isolated. By comparing results from cells in-brine with cells in-supercooled seawater, we can specifically elucidate the impact that salts alone have on microbial activities at a given temperature and without ice formation. This controlled analysis removes the factor of the ice itself, as examined in previous in-ice experimental studies (e.g., Junge *et al*., 2006; Nunn *et al*., 2015) or field work (e.g., Junge *et al*., 2004), where it is impossible to distinguish between effects of temperature and salinity - since in the natural habitat of sea ice both are always intricately linked. Although past work has characterized the effects of temperature and time on psychrophilic activities and proteomes in ice (Nunn *et al*., 2015), to our knowledge the functional responses unique to temperature, salinity and nutrients in *Cp*34H have yet to be characterized.

In this study, *Cp*34H was incubated for 4 months at two subzero temperatures within its growth range, in supercooled seawater or in equilibrium brine, with or without nutrient additions. By tracking bacterial cell counts, metabolic activity, culturability and proteomic responses in tandem across the eight conditions, we investigated proteome shifts to determine potential protein indicators for identifying present or extant life in each independent condition, whether on Earth or other icy worlds. Individual and interactive effects of temperature, salinity and

nutrient availability were disentangled, providing the molecular details of cellular culturability maintenance after extended periods of time. We furthermore analysed the detected peptides from *Cp*34H held at −10°C for 4 months for short polypeptide enrichments to determine if specific amino acids were enriched relative to the entire predicted proteome, representing abundant temperature- or salinity-dependent biomarkers with high detectability and survivability that are compatible with life on Earth found in environments analogous to those proposed off-Earth. As proteins and amino acids survive in the environment for extended periods of time and have been detected in extraterrestrial bodies (e.g., McKay *et al*., 1996; refs within Cobb and Pudritz, 2014; McGeoch *et al*., 2020), we propose and provide a list of short three or four amino acid long polypeptides (referred to as 3- and 4-mers) as candidate biomarkers for future exobiology missions—especially relevant given that most worlds in the solar system are at temperatures well below the freezing point of water with high salinity and limited water activity (Carr *et al*., 1998; Khurana *et al*., 1998; Hand *et al*., 2009; Hendrix *et al*., 2018; Parro *et al*., 2016).

Results

Culturability, abundance and activity analysed after 1 month incubation

Incubations of *Cp*34H (Fig. S1; Dataset S1) in artificial seawater (ASW; Table S2) with nutrient media at optimal salinity and warmer temperature (−1°C) demonstrated that *Cp*34H can grow in this media as indicated by the increase in culturability (quantified as the number of culturable cells determined through MPN technique; see experimental procedures below) over time up to a maximum of 1.45×10^8 cells ml^{-1} (Fig. 1). When incubated at −5°C in supercooled ASW, *Cp*34H maintained a high number of culturable cells ($\sim 1 \times 10^8$ cells ml^{-1}) over 4 months in experiments where nutrients were present (Fig. 1A). Exposure to lower temperature (i.e., −10°C, Fig. 1B and D) resulted in a complete elimination of culturable cells; higher salinity (i.e., 8.4% [for the nutrient-depleted treatment only], Fig. 1C) resulted in a sharp decrease in the number of culturable cells (down to an average of $5.38 \times 10^1 \pm 1.08 \times 10^2$ cells ml^{-1}). With the exception of most of the −10°C treatments, culturability in brine samples increased in the presence of nutrients. Cells remained culturable after 1 month of incubation in −10°C brine treatments, with total cell abundances as high or higher than in −5°C incubations (Fig. S2). Total cell abundance in −5°C brine treatments after 4 months showed a significant decrease ($P < 0.01$; Fig. S2).

[3H]-leucine incorporation into *Cp*34H was tracked for the first month of the incubation and used to approximate the rate of oxygen depletion within the cultures, not accounting for possible oxygen flux into or out of the sealed 1.5 ml eppendorf tubes as the microcentrifuge tubes were likely not gas tight (Table 1; Dataset S3). Generally, *Cp*34H incorporated [3H]-leucine into newly made proteins at both temperatures, usually peaking at 1 h (Table 1). Incorporation rates ranged from 3.63×10^{-7} (−10°C, brine^{-nutr}) to 2.37×10^{-2} (−5°C, ASW^{+nutr}) g bacterial carbon produced per g bacteria carbon per hour, with incorporation rates in ASW two to five orders of magnitude higher than those from corresponding brine treatments (Table 1; Dataset S3). At 1 month, brine^{+nutr} at −5°C doubled incorporation of [3H]-leucine; cells incubated in brine at −10°C showed no measurable levels of activity, and all non-brine treatments showed no major change in [3H]-leucine incorporation (Fig. S3).

Proteomes analysed after 4 month incubation

Using mass spectrometry, we identified a total of 2362 proteins (FDR < 0.01) from a combined analysis of all eight modified temperature, salinity and nutrient treated cell states (47 total MS experiments; Datasets S4, S5). Non-metric multidimensional scaling analysis (NMDS) of the relative abundance (normalized spectral abundance factors: NSAF) of all proteins identified in these experimental treatments revealed that temperature, salinity and nutrient additions drive clustering of MS experimental results on bioreplicates into distinct groups (Fig. 2). Importantly, sub-populations with unique protein profiles emerge after 4 months compared to the *Cp*34H −1°C controls (Fig. 2, black), despite very low levels of metabolic activities and culturabilities in some of the incubations (Table 1). The supercooled ASW samples separate along NMDS component 2, with clusters of −5°C separated by the presence/absence of nutrients. Brine^{+nutr} samples exhibit the greatest separation from the other samples along NMDS component 1 (Fig. 2). Samples incubated at −10°C cluster together in a subpopulation independent of salinity (Fig. 2, red). Immediately adjacent to this cluster are samples from the −5°C brine^{-nutr} condition (Fig. 2).

Growing and maintenance activity signatures of culturable cell populations at −5°C

Analysis of the set of proteins shared between conditions identified 874 proteins common among all groups (Dataset S6). A total of 68 proteins found within the control were not observed in any of the other treatments at 4 months (Fig. 3B, black), whereas 16 proteins were shared among all treatments at 4 months (Fig. 3B, red), indicative of a time- and/or temperature-dependent

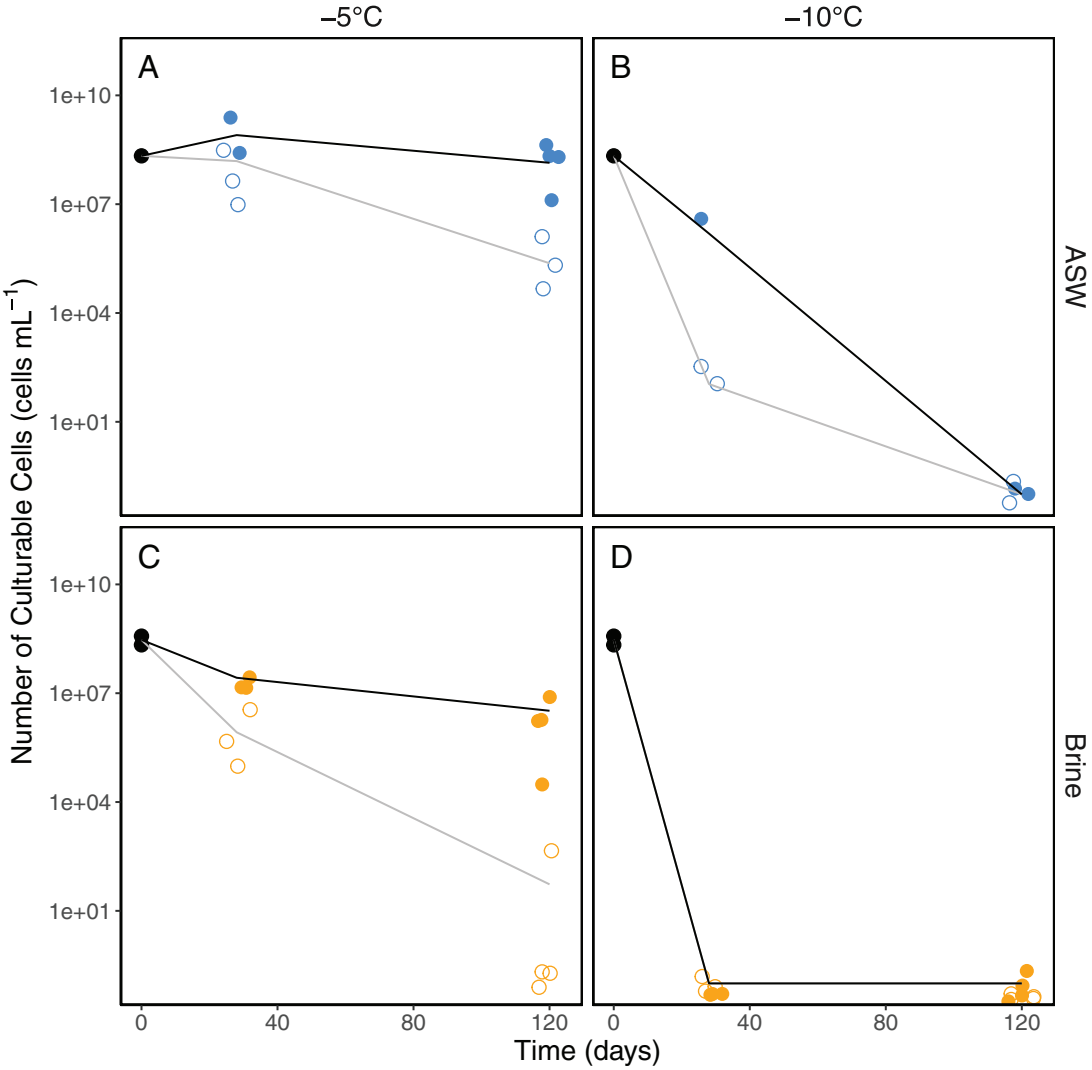

Fig. 1. Most probable number (MPN) of culturable cells (logarithmic scale) after incubation for 1–4 months at −5°C or −10°C. Open symbols indicate cells incubated in saline solution without nutrients (either ASW: blue, −5°C brine or −10°C brine: orange); filled symbols indicate cells incubated in saline solutions amended with nutrients. Black filled circle indicates initial starting condition cell cultures. Lines connect average values at each time point ($^{+nuts}$: black, $^{-nuts}$: grey). Note that the salinity of brines is different for each temperature (see Table S1). [Color figure can be viewed at wileyonlinelibrary.com]

Table 1. Rates and metabolic states of *Cp*34H across experimental treatments.

Temp. (°C)	Condition	Time (h)	Max Rate* gC·gC^{-1} h^{-1}	Oxygen status at 4 months[a]	Metabolic state**
−5	ASW^{-nutr}	2	3.64×10^{-4}	Depleted	Maintenance
−5	ASW^{+nutr}	1	2.37×10^{-2}	Depleted	Growth
−5	brine^{-nutr}	1	7.51×10^{-6}	Limited	Maintenance
−5	brine^{+nutr}	1	4.71×10^{-4}	Depleted	Maintenance
−10	ASW^{-nutr}	1	6.51×10^{-4}	Depleted	Maintenance
−10	ASW^{+nutr}	1	1.59×10^{-2}	Depleted	Growth
−10	brine^{-nutr}	1	3.63×10^{-7}	Limited	Survival
−10	brine^{+nutr}	24	1.47×10^{-4}	Unknown	Maintenance

Maximum [3H]-leucine incorporation rates were calculated from [3H]-leucine uptake and scaled to bacterial abundance according to the methods and values used in Simon and Azam (1989), with an isotope dilution of 126 for nutrient samples and assuming 65 fg C bacterium^{-1} following Junge and colleagues (2006). Metabolic states were derived from the findings of Price and Sowers (2004), assuming a value of 1×10^{-3} for μg for both temperatures listed.
[a]Oxygen depletion rates calculated in Supplemental Dataset S3.

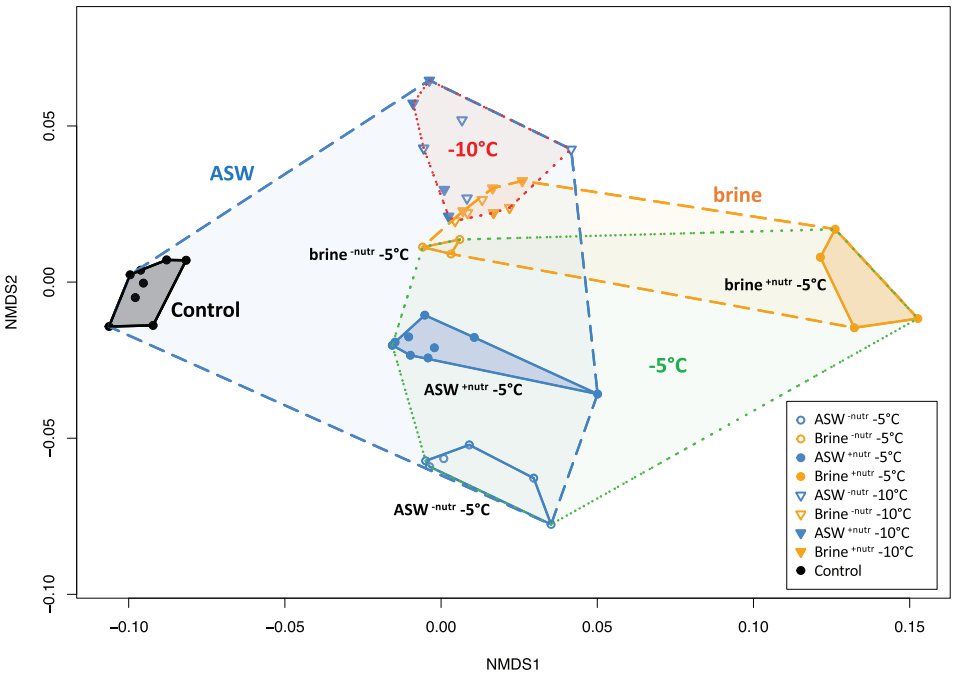

Fig. 2. Non-metric multi-dimensional scaling analysis (NMDS) of the NSAF values for all proteins confidently identified in each bioreplicate from each experimental condition harvested at 4 months. Sample clustering and culturability driven by condition. Open symbols indicate cells incubated in saline solution without nutrients (either ASW: blue, −5°C brine or −10°C brine: orange); filled symbols indicate cells incubated in saline solutions amended with nutrients. Black filled circles represent −1°C starting cell culture conditions (controls). Clustering reveals subgroups based on temperature (dotted line, −5°C: green, −10°C: red), salinity (dashed line, ASW: blue, brine: orange), or salinity-nutrient nexus at −5°C (solid line, colour respective to salinity). [Color figure can be viewed at wileyonlinelibrary.com]

response. The second highest number of unique proteins shared were present in the control, ASW^{+nutr}, ASW^{-nutr} and brine^{-nuts}. Brine^{-nuts}, the condition experiencing the most external stressors, had 45 proteins shared with the control and 12 proteins unique to the condition, the highest abundance of proteins unique to any individual experimental group (Fig. 3B).

The four treatment conditions yielded proteomes distinct from the control (Fig. 4, clusters 1, 4–5, 7–9; Dataset S7–S9). Vertical clustering of protein abundance (NSAF) in the five different treatment conditions revealed that nutrient status controlled the resulting proteome to a greater extent than salinity (i.e., brine vs. ASW), though both ASW samples were more similar to the control than brine samples with the same nutrient status (Fig. 4). ASW^{+nutr} had the second greatest number of proteins observed, which included a variety of proteins involved in nitrogen regulation and iron transport (Fig. 4, cluster 3; GlnK, GlnG, NrtA, NirB and NasA and 4 iron complex outer membrane transport proteins: Fe-Omp). Clusters 4 and 11 are primarily driven by the brine^{+nutr} treatment proteome, with multiple general stress response proteins differentially abundant in cluster 11, including Hfq and CPS_3912 (Fig. 4). Two proteins involved in the generation of exopolymers are represented in cluster 5 (Fig. 4, cluster 5; ExbB, Wza). Cluster 9 consisted of multiple enzymes involved in metabolism and synthesis of secondary metabolites (e.g., AceK, HepA, TypB, ACSL) and in nucleotide metabolism (PpnN, WecB). Brine^{-nutr} contained one protein with a distinct increase in abundance compared to all other conditions: CPS_3809 is a type IV pili methyl-accepting chemotaxis transducer N-terminal domain-containing protein (Fig. 4, cluster 10).

Around 300 proteins in both ASW treatments and around 200 proteins associated with both brine treatments were significantly more abundant relative to controls respectively (Fig. 5; Table S3). The majority of the proteins that increased in abundance were attributed to energy production, amino transport and metabolism processes (Dataset S8). Compared to the two brine states, ASW had a greater number of proteins involved in transcription and cell wall biogenesis (Fig. S4). ASW^{+nutr} had twice as many enzymes increase in abundance (17 vs. 7) involved in carbohydrate transport and metabolism, while ASW^{-nutr} had twice the number of proteins involved in lipid metabolism significantly increase (13 vs. 6, Fig. S4; Dataset S8). Brine^{+nutr} was observed to have over four times the number of significant proteins decrease in abundance compared to all other conditions (489 total, 193 unique, Table S4), representing the functional categories amino acid transport and metabolism (69), energy production and conversion (52), translation, ribosomal structure and biogenesis (35), and function unknown (85; Fig. S4; Dataset S8).

Short polypeptides indicative of high salinity or extreme low temperature

After 2 months, samples incubated at −10°C maintained similar cell counts to those incubated at −5°C despite a complete loss of culturability (Fig. S2). We investigated if

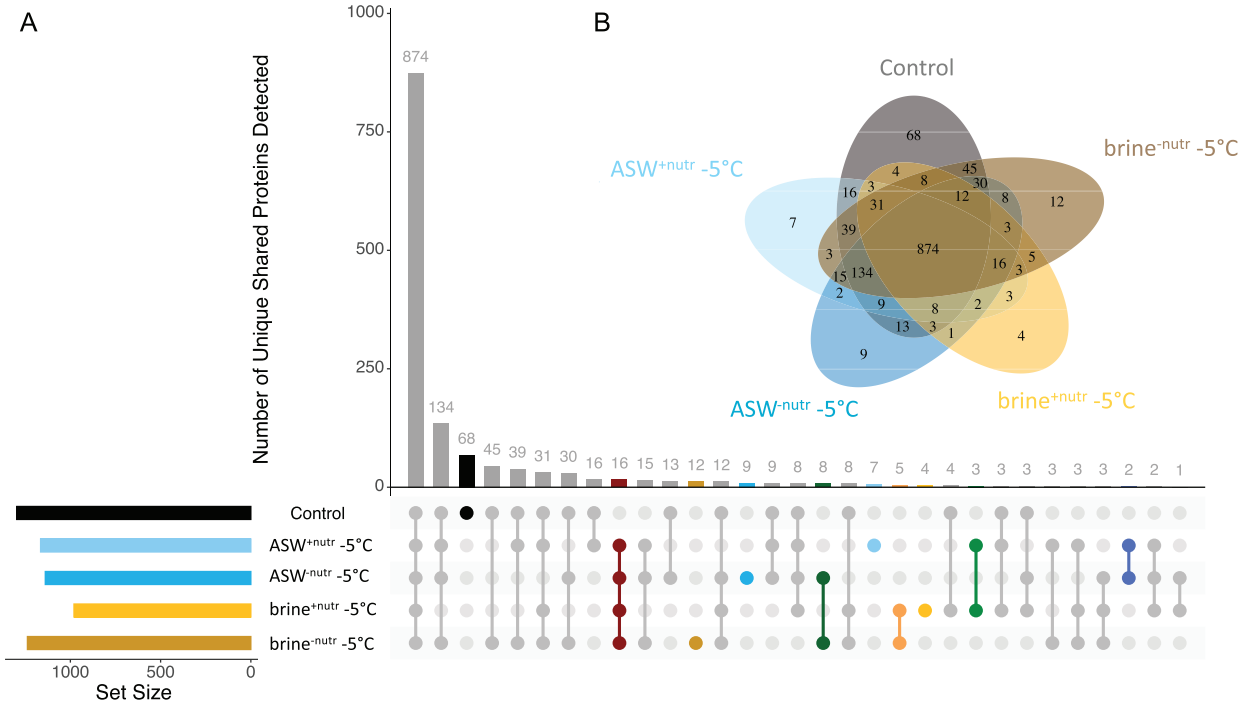

Fig. 3. Visual analysis of quantitative proteomic data identifying unique and shared proteins across experimental conditions. A. Upset plot revealing the number of proteins uniquely shared between the conditions indicated on the parameter grid. The horizontal bar chart on the left represents the number of proteins present in each condition (Set Size). The parameter grid indicates which conditions share unique detected proteins as presented in the vertical bar chart. Parameter grid colours indicate intersections of proteins unique to the control (black), all experimental conditions (red), ASW-specific conditions (blues), brine-specific conditions (yellow and oranges), and unique to nutrient additions (greens). B. Venn diagram revealing the overlap and uniqueness of proteins identified across all samples. [Color figure can be viewed at wileyonlinelibrary.com]

specific 3–4 amino acid-long polypeptide combinations ('k-mers') indicative of the individual stressors of extreme low temperature (−10°C), high salinity (brine), or the co-occurrence of these stressors accumulate in extremophile cells. ANOVA analysis of the semi-quantitative proteomic data from the −5°C and −10°C treatments identified unique sets of proteins specifically associated with extreme low temperature (885 proteins), high salinity (586 proteins) and the interaction of the two stressors (1802 proteins) at a 1% FDR threshold.

In general, there were fewer temperature-specific k-mers (79) than brine-specific k-mers (180, Fig. S5A; Dataset S10). Proteins identified to be significantly increased in the −10°C brine treatments contained the highest number of unique enriched k-mers (367, Fig. S5A; Dataset S10). Temperature-specific 3-mers in −10°C conditions were significantly enriched in glutamic acid (E) and valine (V), while aspartic acid (D) and threonine (T) were depleted relative to all other detected protein k-mers (Table S5). The distributions of amino acids were not significantly different in the temperature-specific 4-mers (Table S5). Salinity-specific 3-mers in brine conditions were significantly enriched in alanine (A) and depleted in aspartic acid (Q) relative to all other detected protein k-mers (Fig. S5B; Table S5). The distributions of amino acids in brine-specific 4-mers also had significantly higher frequencies of alanine (A), but also higher abundances of the polar amino acid glutamine (Q; Table S5). These brine-specific 4-mers were likewise depleted in aspartic acid (D) and the two non-polar amino acids phenylalanine (F) and tryptophan (W; Fig. S5B; Table S5).

One k-mer, *Lys-Asp-Ala* (KDA), was identified to be enriched in each of the three isolated analyses of extreme low temperatures (−10°C), high salinity (brine), and a combination of both (−10°C brine) responses (Fig. S5A; Dataset S10). The four k-mers that were identified to be enriched in the brine and −10°C treatments separately, but not in the co-occurring stressor treatment, were dominated by the presence of alanine*: Val-Glu-Gly, Glu-Ala-Ala, Ala-Ala-Gly and Lys-Ala-Ala* (VEG, EAA, AAG, KAA; Fig. S5A). Analysis of shared k-mers between the high salinity and the combined high salinity and low temperature treatment revealed 19 k-mers. Of the 534 4-mers identified to be enriched in the proteins inferred from our peptide data, 96% (512) of them were actually detected by mass spectrometry in our condition-specific samples.

Fig. 4. Vertically and horizontally clustered heatmap view of all proteins revealed to be increased in abundance in one of the four treatment conditions at −5°C (ASW^{+nuts}, $brine^{+nuts}$, ASW^{-nuts}, $brine^{-nuts}$) relative to the control condition by $\log_2$ fold ≥2 ($P < 0.05$). Vertical dendrogram indicates hierarchical clustering of the different samples, while horizontal dendrogram clustered protein NSAF values normalized by row (12 clusters, 118 proteins). [Color figure can be viewed at wileyonlinelibrary.com]

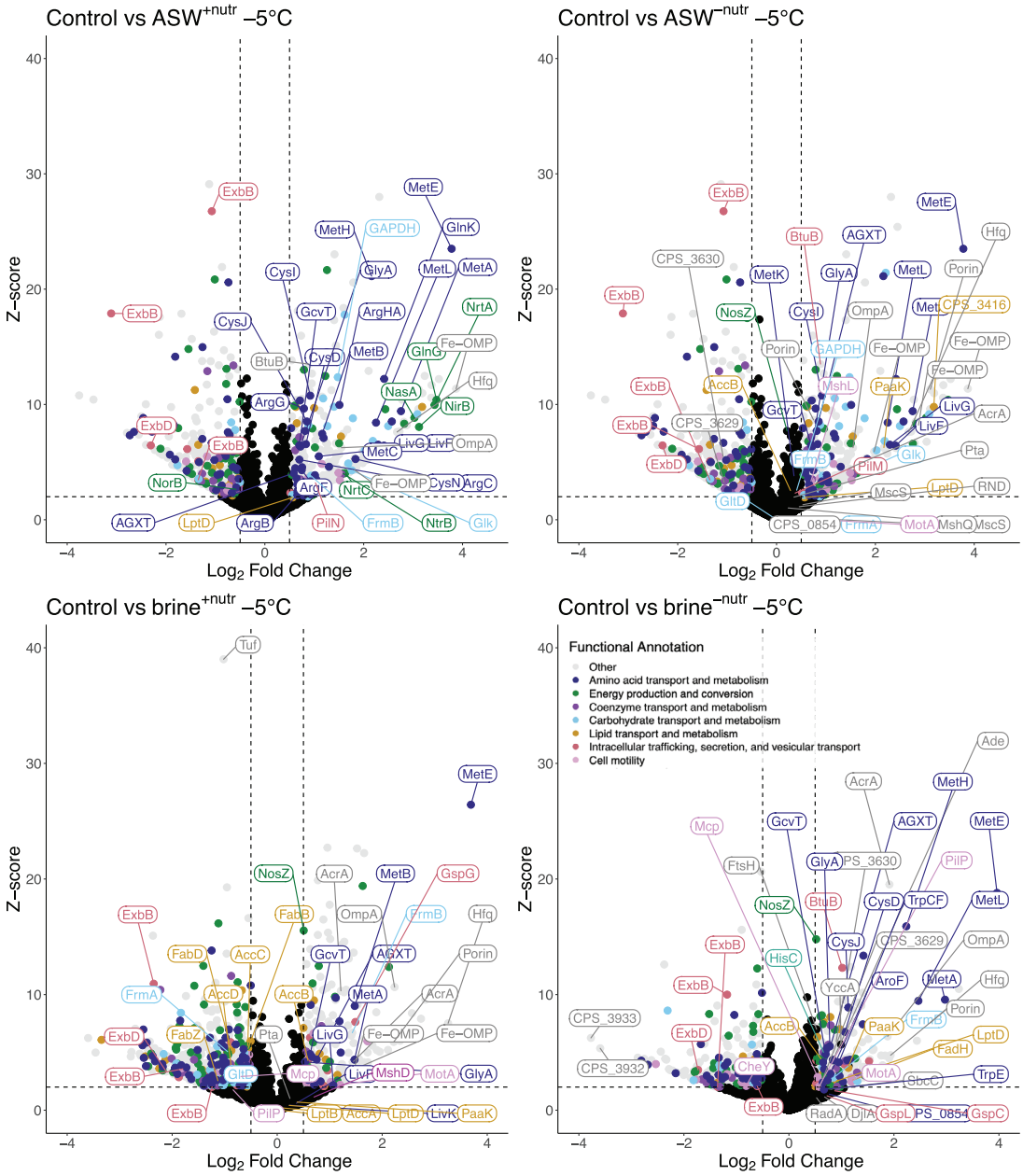

Fig. 5. Differential abundances (log_2 fold change: LFC) of all proteins detected in four experimental –5°C conditions compared to control cells and their respective significance z-score calculated. Average protein abundances were determined from spectral counts from the control samples and compared to the average spectral counts for the experimental conditions: A. ASW^{+nuts}; B. ASW^{-nuts}; C. $brine^{+nuts}$; D. $brine^{-nuts}$. Proteins meeting a significance threshold of LFC ≥ |0.5| and a z-score ≥ 2 are indicated in colour where each colour represents a different EggNOG term. Functional annotations are: dark blue: amino acid transport and metabolism, green: energy production and conversion, magenta: coenzyme transport and metabolism, light blue: carbohydrate transport and metabolism, orange: lipid transport and metabolism, dark pink: intracellular trafficking secretion and vesicular transport, light pink: cell motility. Proteins were labelled with a protein name if the LFC ≥ |2| or z-score ≥ 15. [Color figure can be viewed at wileyonlinelibrary.com]

Discussion

Culturability and activity analysis

As is the case for sea ice (when bacterial cells get included into recently formed ice immediately experiencing a change in salinity and temperature in their new habitat), cells of *Cp*34H were immediately transitioned from control conditions into their respective media destined for long-term incubations without any prior acclimatization steps. As shown previously for in-ice incubations (Junge *et al*., 2006; Nunn *et al*., 2015), *Cp*34H is capable of withstanding this rapid transition into subzero

solutions, evidenced by positive measures of incorporation of [3H]-leucine (i.e., protein synthesis) at rates that indicate that cells in the majority of treatments were in metabolic states of either growth or maintenance by 24 h (metabolism-terms according to established rates in Price and Sowers, 2004; Table 1; Fig. S3). The only exception was −10°C brine^{-nutr}, with an activity rate representative of a physiological survival state (Table 1). Here, we characterize the response of *Cp*34H after 1 month incubation as being in one of four physiological activity states: (i) growing and culturable cells (high levels of activity and culturability; −5°C, ASW), (ii) active cells (low levels of activity and moderate culturability; −5°C, brine), (iii) viable but not culturable, or VBNC, cells (moderate levels of activity and very low to no culturability; −10°C, ASW^{-nutr}) and (iv) surviving cells (very low to no levels of activity and not culturable but persisting as evidenced by maintained total counts; −10°C, brine).

Throughout this paper, we chose to use the term culturability as an assessment of cell state as it most accurately reflects what is being measured in our samples. In the literature, culturability has also been used synonymously with viability, alluding to the fact that cells must be viable in order to be amenable to culturing (Pinto *et al*., 2015). For many bacterial species, as was the case in our study, cells can still be viable (as indicated by positive measures of [3H]-leucine based protein synthesis) but not culturable (as indicated by no recoverability in culture). This cell state, referred to in the literature as the VBNC (Viable But Not Culturable) cell state, has been described as a survival strategy for cells coping with environmental stress without entering dormancy (Pinto *et al*., 2015; Ayrapetyan and Oliver, 2016). Evidence of the VBNC state in our −10°C ASW^{-nutr} samples at 1 month warrants further study, especially in view of the fact that a better understanding of this adaptive strategy may help inform future astrobiological searches, particularly given the relevance of maintaining a measurable level of activity that ensures long-term survival in salty and super cold environments such as might be found on other icy worlds.

Our finding of continued protein synthesis activity at −10°C in supercooled ASW, but not in high salinity brine, suggests salinity stress as the most detrimental factor under the conditions studied here. This is congruent with the known growth salt content range of *Cp*34H ([1.5%–7.0%, in marine medium], Huston, 2004), and the fact that cells were not culturable after 1 month of incubation in −10°C brine. After 4 months at −10°C, cells in all treatments were unculturable (Fig. 1), suggesting that both the lower temperature and the higher salinity affected culturability to a greater degree after prolonged incubation. Organisms frozen in sea ice at −10°C are expected to be partitioned in the brine fraction of the ice (Junge *et al*., 2019), and thus experience conditions equivalent to those of our −10°C equilibrium brine treatments (Fig. 1D). Our data suggest that *Cp*34H would not be active under the more extreme temperature and salt content conditions within 1 month of incorporation into sea ice. However, natural wintertime sea ice samples are known to contain an abundant supply of potentially cryo- and halo-protective exopolymers thought to be important for microbial survival (Krembs *et al*., 2002; Krembs and Deming, 2008; Krembs *et al*., 2011) and in-ice activity (Junge *et al*., 2006), and it is possible that *Cp*34H remains active when embedded within such substances in the ice (Junge *et al*., 2006; Marx *et al*., 2009). Further studies that include polymer amendments could shed light on the likelihood of active growth in high salinity brines of *Cp*34H with significance for sea ice environmental conditions.

The dynamic proteomic response of Cp34H in subzero temperatures

The predicted proteome for *Cp*34H consists of 4910 proteins (Methé *et al*., 2005), of which we identified 2362 proteins (48% of the predicted proteome). This expands on previous studies by Nunn and colleagues who identified 1763 proteins (36%; Nunn *et al*., 2015). Technical and biological replicates of proteomic signatures from each condition form distinct subpopulation clusters in an NMDS analysis, providing confidence that the 4 month-long treatments yield distinct protein responses based on temperature, salinity and nutrients in *Cp*34H (Fig. 2). Because samples at −5°C retained culturability (Fig. 1A and C), these proteins were analysed to provide information about how active cells mitigated decreased temperature, increased salinity and nutrient limitation; samples at −10°C, which lost culturability but contained persisting cells (Fig. 1B and D; S2), were analysed for the enrichment of polypeptides that could serve as biomarkers for previously active life on icy worlds.

Constitutive proteomic response of Cp34H to 4 month exposures of −5°C

The constitutive proteomic response from *Cp*34H suggested a metabolic shift toward an anaerobic-like state through the increased expression of proteins involved in the Entner–Doudoroff pathway (Czajka *et al*., 2018) and sulfate reduction (Parro *et al*., 2016; Fig. 5A–D). The alteration of these central core metabolisms in 4 month-long incubations support calculations and previous suggestions that the cellular chemical reactions in these pathways occur more spontaneously (i.e., more negative value calculated for Gibbs free energy) than traditional C, N and S acquisition (Flamholz

et al., 2013; Noor *et al*., 2014; Czajka *et al*., 2018). Observed increases in amino acid transport across all conditions emphasizes the rapid response of these cells to the available extracellular substrates (i.e., free leucine) and intracellular recycling of amino acids as a primary nitrogen source. In particular, cysteine and methionine metabolism, a metabolic source of sulfur and nitrogen, were observed to increase in all conditions. Additionally, proteins involved in cellular motility, including flagellar, pilus and chemotaxis proteins, were abundant across all conditions, supporting previous examinations of *Cp*34H in response to subzero temperatures (Nunn *et al*., 2015; Showalter and Deming, 2018) and presenting additional motility-specific biomarkers for extant life as desired by NASA's Ladder of Life Detection (Neveu *et al*., 2018).

Responses to temperature, salinity and nutrients

Our analysis of the proteins that significantly diverge in critical metabolic pathways of each condition at −5°C in comparison to the control identified unique mitigation strategies in each individual treatment. These condition-specific analyses revealed that the availability of nutrients triggered the use of new pathways of carbon and nitrogen assimilation and the additional stress of low temperatures or high salinity initiated intracellular recycling to strengthen cell walls. In addition to analysing each individual condition, a broader analysis of environmental variables was performed to isolate effects of salinity, nutrients and temperature on *Cp*34H.

ASW with nutrients. Cells incubated in ASW^{+nutr} at −5°C experienced conditions closest to the −1°C control, allowing for an isolated examination of long-term temperature- and reduced available oxygen- dependent effects. The reported growth range for *Cp*34H extends from 19°C to −12°C, with an optimal growth temperature of 8°C (Junge *et al*., 2003; Huston, 2004; Wells and Deming, 2006a, 2006b). Within the context of this range, we hypothesize that *Cp*34H experiences minor temperature stress, not enough to permanently damage cells, but enough to activate metabolic pathway networks within the cell that lead to an optimized maintenance of functionality. At −5°C, cells were able to maintain levels of culturability equivalent to that experienced by cells in optimal conditions (Fig. 1A). Activity as measured by the maximum incorporation rate of [3H]-leucine after 1 h was also observed at rates (2.37×10^{-2} gC·gC^{-1} h^{-1}) consistent with either growing or metabolically active cells (Price and Sowers, 2004; Junge *et al*., 2006; Table 1).

The predominant mitigation strategy of −5°C ASW^{+nutr} to withstand long-term incubation was the increased utilization of amino acid metabolism (Figs. 5A and S4), facilitated primarily by mechanisms of assimilatory nitrate reduction described herein, that allowed *Cp*34H to preserve activation of necessary pathways for maintaining cell activity over prolonged time frames (Fig. 4). An increased production of amino acids in ASW^{+nutr} requires a readily available nitrogen source. Though it is difficult to ascertain if cells in ASW^{+nutr} were nitrogen limited by month four, the increase in abundance of nitrogen regulatory proteins, including nitrate ABC transporter (NrtA), nitrate reductase (NasA), nitrite reductase NADPH (NirB), nitrogen regulatory protein PII (GlnK) and DNA-binding transcriptional regulator NtrC (GlnG; Fig. 4, cluster 3; Fig. S6), suggests *Cp*34H modulates its need for nitrogen through the directed acquisition of extracellular nitrate, a predominant and readily available form of nitrogen shown to drive biogeography and trophic status in Arctic surface waters and sea ice (Ardyna and Arrigo, 2020; Clark *et al*., 2020; Henley *et al*., 2020). Notable nitrate transporters included NrtA, an ABC transporter responsible for high-affinity nitrate acquisition at low concentrations (Nagore *et al*., 2006; Akhtar *et al*., 2015), and GlnG, a component of the NtrB/NtrC system that responds to nitrogen limitation and plays an important role in the regulation of transcription (Pahel *et al*., 1982). *Cp*34H's preferential expression of high-affinity transporters in this analysis suggested that the initial nutrient concentration supplied did not sustain the metabolic needs of the cells over the entire 4 month incubation, possibly due to ASW^{+nutr} at −5°C possessing the highest rates of activity during early time point measurements (Table 1). Other notable nitrogen metabolism proteins increased in ASW^{+nutr}, such as nitrate reductase (NasA) and nitrite reductase NADPH (NirB), suggested that *Cp*34H may utilize assimilatory nitrate reduction pathways for producing ammonia (Fig. 4, cluster 3; Fig. S6). For example, *Mycobacterium tuberculosis* incubated under hypoxia conditions was able to utilize nitrite as a sole nitrogen source due to NirB, an iron–sulfur containing protein that can reduce nitrite directly to ammonia (Jackson *et al*., 1981; Wang and Gunsalus, 2000; Chen and Wang, 2015), allowing critical nitrogen regulation when cells entered dormancy states (Akhtar *et al*., 2013). This assembly of proteins emphasized the benefits of metabolic diversification in nitrogen regulation in the dual presence of low temperature and potential reduced oxygen stress.

In close relation to nitrogen metabolism, ASW^{+nuts} uniquely revealed increased abundances of enzymes involved in arginine biosynthesis, while all other conditions decreased the abundance of these enzymes (Fig. S7). Previous studies have suggested psychrophiles reduce arginine content in proteins because of increased hydrogen bonding and reduced protein flexibility (De Maayer *et al*., 2014), while other studies have revealed that marine psychrophiles grown with readily available nutrients, such as this, use chemotaxis and active

transport to acquire and assimilate arginine (Geesey and Morita, 1979). Arginine can be utilized in the biosynthesis of glutamate and evidence here supports the hypothesis that glutamate is being synthesized from the abundant branched-chain amino acids (Wu and Morris, 1998; Fig. 5A, putative branched chain amino acid transporters: CPS_3416, CPS_3412/LivF, CPS_3417/LivG). Significant increases in GlnK, a component of the nitrogen regulatory protein PII, also suggested that cells tightly regulate acetyl CoA and arginine metabolism (Watzer *et al*., 2019; Dataset S7). Overall, these preferential mechanisms of nitrogen regulation through nitrate reduction proteins and arginine biosynthesis pathways allow ASW^{+nuts} to maintain a wide array of metabolisms that sustain its high culturability over 4 month incubations at a decreased temperature.

ASW without nutrients. In the Polar oceans, nutrient levels vary widely, have changed considerably with the climate change pronounced there, and show low and high nutrient conditions occurring at different locations or at different times of the year (Ardyna and Arrigo, 2020; Henley *et al*., 2020). In cold, nutrient-depleted waters, organisms require multiple strategies for nutrient acquisition and cold-response maintenance for long in-ice residence times. In our incubations, the one order of magnitude reduction in culturability of cells observed in ASW^{-nutr} compared to cells in ASW^{+nuts} indicated that the presence of nutrients plays a critical role in maintaining higher levels of culturability under subzero conditions (Fig. 2), confirming the widely accepted hypothesis that psychrophilic growth is enhanced with increased nutrient availability (Moyer *et al*., 2017). Primary drivers of metabolism in ASW^{-nutr} included modifications to the membrane through the regulation of two-component systems, increases in membrane receptors and alterations to fatty acid metabolism (Fig. 5B, Figs. S4 and S8).

The major membrane proteins substantially increased were TonB receptors, with 12 enzymes (i.e., TonB, ExbB, ExbD and Fe-OMP iron complex outer membrane receptors) discovered to have a significant $\log_2$ fold change in ASW^{-nutr} (Fig. 5B; Dataset S9). TonB receptors are active transporters that facilitate uptake of a wide range of molecules and nutrients (i.e., vitamin B12, siderophores, polysaccharides, aromatic compounds (Pawelek *et al*., 2006; Shultis *et al*., 2006; Bolam and van den Berg, 2018; Fujita *et al*., 2019)). TonB is part of a membrane complex that includes ExbB and ExbD proteins; in our data, these proteins were observed to decrease significantly in all conditions compared to the control cells (Fig. 4; Dataset S9). As extracellular polysaccharides (EPS) play a key role in stabilizing extracellular environments for *Cp*34H and other psychrophiles (Bowman, 2017; Deming and Young, 2017), it was interesting that despite TonB receptors being significantly increased, ExbB and ExbD are only increased in control conditions (Fig. 4; Dataset S9). This may be a time-dependent expression, suggesting that EPS is already present in the cell matrix and does not need to be remade through the 4 month incubation. Notably, several other membrane proteins were observed to significantly increase in ASW^{-nutr} (12 efflux pumps: RND, Acr family A/B/D/E/F, magnesium CorC and cobalt; 9 type IV pilus biogenesis proteins: Pil-N/O/C/P/M/Q, MshL; 2 Omp porins; 4 mechanosensitive ion channel proteins; Fig. 5B; Dataset S9). These membrane modifications may serve to aid cells in their acquisition of extracellular nutrient sources through control of membrane permeability or nutrient depletion-directed motility (Ferenci, 2005; Castillo-Keller *et al*., 2006; Ni *et al*., 2016).

Additionally, the existence of proteins from both biosynthesis and degradation pathways in fatty acid metabolism suggested that long-chain fatty acids were constructed or deconstructed as needed, confirming the critical importance of adapting membrane fluidity for maintaining activity at low temperatures (Bowman, 2017). Specifically, lipopolysaccharide (LPS) assembly protein LptD was increased, along with AccB, an acetyl-CoA carboxylase that leads to the production of malonyl-CoA (Fig. 5B). Malonyl-CoA signals bacteria to increase their production of fatty acids and phospholipid biosynthesis by acting as a potent negative regulator of fatty acid catabolism (Fujita *et al*., 2007). Additionally, increases in fatty acid degradation proteins FadB and FadE were offset by the presence of FadR, a regulator for fatty acid metabolism (Fujita *et al*., 2007; Zhang *et al*., 2012). *Cp*34H encodes multiple copies of various fatty acid metabolism regulatory proteins in its genome (Wan *et al*., 2016), emphasizing the need for high-precision regulation for the utilization of fatty acids in diverse environments. The increase in fatty acid biosynthesis enzymes, even in the absence of external nutrients, showed that (i) *Cp*34H has multiple methods for coping with nutrient limitation, (ii) cells are adept in balancing multiple external stressors and (iii) the combination of the more moderate temperature and nutrient stresses tested here are not enough to engage the prioritization of fatty acid breakdown, thus showing that cells are prepared to handle more extreme conditions than those in ASW^{-nutr} incubations.

Brine with nutrients. Shelf Arctic ocean waters are fed by nutrient-rich sources (Torres-Valdés *et al*., 2016), and brine inclusions within land-fast sea ice are often respectively nutrient replete, offering a variety of extracellular substances for organisms residing in such inclusions to utilize for prolonged survival. Some of the metabolites captured in brine inclusions contain classes of compatible

solutes that can serve as osmoprotectants against the increased salinity imposed by the brine as the ice ages (Welsh, 2000; Firth *et al*., 2016). The slight decrease in culturability in brine^{+nutr} (Fig. 1C) reflected an expansive salinity and growth response that decreased both the diversity and abundance of proteins detected (Fig. 5C; Table S4), yielding the most distinct matrix of proteins tested in this study (Fig. 2). Of the four conditions at −5°C, brine^{+nutr} had the lowest number of unique proteins (Fig. 3, yellow) and the highest number of proteins significantly decreased in abundance compared to the control, independent of functional category (Fig. 4C; Table S4). Large decreases in ribosomal subunits were observed that were not apparent in other conditions (Fig. S9), suggesting that part of the overall decrease in protein abundance is due to the lack of available cellular machinery for engaging in translation. The general decrease observed in both protein count and abundance detected compared to other conditions suggests that brine^{+nutr} cells increased protein turnover in order to prioritize a subset of enzymes to survive the increased salinity exposure (Fig. 4).

Potential protein biomarkers of salinity stress observed in this study are Hfq, OmpA and type IV pilus proteins (Fig. 5C and D). The most notable protein contributing to these changes is Hfq, a stress-activated RNA-binding chaperone protein that directs a profound number of biological processes in bacteria including carbon metabolism (Vogel and Luisi, 2011), fatty acid biosynthesis (Bianco *et al*., 2019; Huber *et al*., 2020), chemotaxis and motility (Soutourina and Bertin, 2003) and membrane proteins (Deng *et al*., 2016). Hfq had the second highest increase in log fold change (Fig. 5C) in brine^{+nuts}; while Hfq was detected as increased at high levels in all experiment conditions (Fig. 5A–D), the combination of brine and nutrients extends the influence of this RNA chaperone to lead the induction of widespread protein decreases. Because of its increased prevalence with the addition of multiple stressors, Hfq could serve as a potential biomarker for cells in extreme environments. The Hfq gene is required for the regulation of OmpA, an outer membrane protein that is osmoregulated, involved in maintaining membrane integrity (Udekwu *et al*., 2005; Choi and Lee, 2019), and was increased in abundance in brine^{+nuts}. Evidence of increased OmpA in halophilic bacteria supports the use of this protein as an indicator for a prolonged salinity stress response (Yun *et al*., 2018). Additionally, OmpA mRNA is notably stable, which could increase the likelihood of translation under extreme stress (Nilsson *et al*., 1984; Vytvytska *et al*., 1998, 2000). The increase in type IV pilus protein MshD, 1 of 4 proteins uniquely detected in brine^{+nutr} (Fig. 3), reveals a brine^{+nuts} - driven response and may represent a biomarker for psychrophiles in higher nutrient brines. Additionally, a significant increase in branched-chain amino acid ABC transporters was observed both in brine^{+nutr} and ASW^{+nutr} conditions (LivG, LivF, LivK, Fig. 4, clusters 2, 3, 4; Fig. S10; Dataset S7), confirming the preferential utilization of leucine, which was provided in our nutrient additions, and thus validating our use of leucine as a protein synthesis tracker for activity assessment (Table 1).

Proteins with the greatest decrease in abundance in brine^{+nutr} were involved in fatty acid metabolism (Fig. 5C, Table S4). Enzymes involved included acetyl-CoA carboxylase carboxyl transferase (AccC/A/D, Fig. 5C) and acyl-carrier proteins (FabG/V/D/B/A/Z/F/Y, Fig. 5C). Brine^{+nutr} was the only condition to induce widespread decreases in fatty acid biosynthesis, though no notable enzymes involved in degradation were detected as significant (Fig. S11; Dataset S7). This indicated that the entire process of fatty acid metabolism has been included in the observed protein decrease experienced. It is possible to infer that cells avoid expending energy on the degradation of fatty acids due to the presence of other utilizable nutrients in their environment that they can acquire through the increased use of type IV pilus proteins. This study reveals that cells experiencing increased salinity in the presence of a readily available nutrient source undergo widespread decreases in metabolism while maintaining select stress proteins that are increased to levels greater than in any other condition.

Brine without nutrients. Bacteria in these subzero, hypersaline environments possess adaptations of great relevance to astrobiology, as the presence of liquid water on icy worlds facing constant extreme cold temperatures is dependent upon an over-saturation of salts (Zolotov, 2007; Dickson *et al*., 2013; Vance *et al*., 2019). As such, proteins increased in these incubations could inform further investigation into valuable biomarkers for life in extreme conditions. In response to varied stressors, brine^{-nutr} cells exhibited the highest number of unique proteins in any experimental group (Fig. 5B and C), including a putative gluconeogenesis factor protein for regulating cell shape (CPS_2836), NAD kinase (NadK) which synthesizes NADP and acts as an essential reducing agent (Spaans *et al*., 2015), an ubiquinone kinase (UbiB) that functions under anaerobic conditions (Meganathan, 2001) and membrane-bound proteins such as an RND efflux- and ATP- transporters that can regulate the ion concentrations within cells (Tokunaga *et al*., 2004; Li and Nikaido, 2009). This diverse set of unique proteins suggests that brine^{-nutr} cells must initiate a suite of metabolic processes to survive cold, high salinity conditions with limited nutrients for extended periods of time. The varied metabolic response of −5°C brine^{-nutr} was only partially effective at maintaining culturability

after 4 months (Fig. 1C), with an NMDS analysis revealing that these samples clustered nearest cells incubated at −10°C which completely lost recoverability (Figs. 1B, D and 2A). Conversely, the comparable condition of ASW^{-nutr}, with equivalent temperature and nutrients, exhibited only a moderate decrease in culturability (Fig. 1A), suggesting that proteins specific to brine^{-nutr} were responsible for conferring increased protection against salinity stress. An increase in enzymes involved in aromatic amino acid metabolism, including activation of the shikimate pathway (AroE, CPS_3954, TrpCF, TrpE, HisC, TyrA, Fig. 5D), have all been previously noted as defence mechanisms against increased salinity (Falb *et al*., 2008; Lee *et al*., 2016).

When cells experienced temperature, salinity and nutrient stress simultaneously (i.e., brine^{-nutr} samples), we detected an increase in the ATP-dependent peptidase FtsH, an important regulator of growth, cell division and extracytoplasmic membrane stress that is also required for the synthesis of multiple components of polysaccharides (Ito and Akiyama, 2005; Fig. 5D; Dataset S9). FtsH is a membrane protein responsible for degrading thermodynamically unstable proteins and maintaining cellular and membrane LPS (Shimohata *et al*., 2002; Ito and Akiyama, 2005). These membrane-specific changes, combined with increases in the FTS negative regulator protein YccA, associated type II secretion system proteins (GspC, GspL, Fig. 5D) and other fatty acid regulation proteins (LptB, DjlA, PaaK, FadH, Fig. 5D), suggest that brine^{-nutr} mitigates the matrix of environmental stressors by actively maintaining a highly regulated, LPS-enriched membrane. Fortified (and specialized) membranes can buffer the cells against the subzero saline environment while simultaneously managing any internal damage to cellular processes via DNA damage repair (SbcC, RadA) and purine salvage pathway proteins (Ade), two processes that are likely correlated with the high salt content of the brine incubation (Fig. 5D). The nutrient-limited state also increases chemotaxis, motility and amidohydrolase proteins common to both nutrient-limited conditions (see *General Nutrient-Limitation Response* below). Additionally, enoyl-CoA hydratase (i.e., PaaK) isolated from the haloarchaea *Haloferax mediterranei* was essential for the mobilization of carbon stored in polyhydroxyalkanoate (PHA) through beta-oxidation pathways also present in *Cp*34H, suggesting a possible recycling of fatty acids for use as a carbon source in brine^{-nutr} (Methé *et al*., 2005; Liu *et al*., 2016).

General salinity-dependent response. In our samples, protein pathways prioritized in response to increased salinity include general amino acid transport and recycling, an intracellular metabolism that would also provide the cell with needed carbon and nitrogen (Fig. S4). OmpA was also prioritized and has been characterized in *Escherichia coli* for its significant role in maintaining membrane integrity. The combined correlation of Hfq and OmpA to cellular envelope stress in high salt conditions suggests a distinct salinity response by *Cp*34H (Fig. 5C–D, Table S4; Choi and Lee, 2019). Additionally, psychrophiles and halophiles have contradictory strategies for the production of branched-chain fatty acids (Ventosa *et al*., 1998; Chattopadhyay, 2006; LivG, LivK, LivF, Fig. 4), therefore *Cp*34H cells exposed to both low temperatures and high salinities must combine strategies, as was observed here. Due to the increased expression of fatty acid biosynthesis proteins (i.e., LptD, LptB, AccB, PaaK, Fig. 5), we also propose that fatty acids be explored for use as potential biomarkers for high salinity candidates. For example, while psychrophiles are documented to increase branched-chain fatty acids (Rotert *et al*., 1993; Chattopadhyay, 2006), halophiles decreased branch-chains in favour of cyclopropane fatty acids and unsaturated fatty acids (Ventosa *et al*., 1998). Because the presence of branched-chain C15 monounsaturated fatty acid is so unusual among halophilic bacteria, Skerratt and colleagues (1991) proposed it as a taxonomic biomarker for specific strains isolated from Antarctic lakes.

General nutrient-limitation response. Entrapment in sea ice brine inclusions would create a closed system, naturally creating a nutrient limited environment. Both ASW^{-nutr} and brine^{-nutr} cells displayed increased abundance of proteins involved in chemotaxis-directed motility (MotA, Mcp, Figs. 5B and D), consistent with previous microscopic evidence that cells actively follow nutrient gradients (Junge *et al*., 2003; Showalter and Deming, 2018). Nutrient-limited treatments also exhibited increases in pilus proteins responsible for *Cp*34H nutrient acquisition (PilP, PilC). Type IV pilus proteins are present in a diverse array of bacteria (Craig *et al*., 2019), aiding primarily in the acquisition of nutrients (Gold *et al*., 2015), suggesting that once detection and abundance thresholds are quantified, they may serve as good biomarkers of generalized nutrient limitation in field work. Additionally, type IV pili possess a twitching motility as well as the ability to sense and adhere to solid surfaces, creating the potential for ice-affine surface adaptations or adhesion to inorganic solutes present within brine channels (Collins, 2009; Baker *et al*., 2017; Craig *et al*., 2019). An increased abundance of amidohydrolase family proteins (CPS_3630, 3629, 0854), which have been associated with increased growth of organisms in nutrient-limited conditions (Cezairliyan and Ausubel, 2017), suggests these hydrolytic enzymes could serve as a general biomarker for low nutrient bioavailability.

General temperature-dependent response after 4 months at −5°C. The general response to a decrease in temperature over 4 months relative to the control culture is primarily characterized by significant changes in carbon metabolism, emphasizing its central role in cell survival as temperature decreases (Czajka *et al*., 2018; Figs. S13–S16; Dataset S9). Proteins in the glycine cleavage system were increased in *Cp*34H, which allowed cells to utilize products, e.g., glycine betaine, as compatible solutes or as bioavailable sources of carbon and nitrogen (Andreesen, 1994; Methé *et al*., 2005; Gunde-Cimerman *et al*., 2018). Enzymes involved in the detoxification of formaldehyde were identified [i.e., S-formylglutathione hydrolase (FrmB), S-(hydroxymethyl) glutathione dehydrogenase (FrmA), alanine-glyoxylate transaminase (AGXT)] highlighting the importance of methane and other small 1-C substrates as a primary carbon source utilized through the folate biosynthesis pathway [i.e., aminomethyltransferase (GcvT), 5-methyltetrahydrofolate-homocysteine methyltransferase (MetH), glycine hydroxymethyltransferase (GlyA)] at the 4 month time point (Denby *et al*., 2016). In nutrient-replete bacterial incubations, it has previously been noted that these metabolisms are initiated after macromolecular carbon sources are depleted (Mikan *et al*., 2020). That said, all conditions possess enzymes for the breakdown of glucose through the Entner-Doudoroff pathway [glucokinase (GLK), glyceraldehyde 3-phosphate dehydrogenase (GAPDH); Figs. S13–S16], indicating either that glucose remained in the system, or these enzymes are retained by *Cp*34H and express slow turnover rates. This same network of carbon metabolism enzymes produce formate, methanol, NADH and hydrogen, all byproducts from precursors previously recognized/modelled to increase in ice veins (Price, 2000). Similarities in carbon metabolism could be due to the utilization of choline as a substrate for energy production and biosynthesis pathways (Collins and Deming, 2013; Czajka *et al*., 2018). Choline, a B vitamin and preferentially utilized osmolyte by *Cp*34H in sea ice brines (Firth *et al*., 2016), would be expected to be present at adequate levels in conditions receiving nutrients due to the inclusion of yeast extract, but it appears that even cells lacking nutrients rely on this pathway for metabolism when other stressors are present.

MetE, a vitamin B12-independent methionine synthase (Mordukhova and Pan, 2013), had the highest $\log_2$ fold change of any protein detected in all conditions (Fig. 5A–D), with the exception of ASW^{+nuts}. Additionally, all conditions except ASW^{+nutr} also exhibited a significant increase in nitrous oxide reductase (NosZ, Fig. 5B and C; Dataset S7), suggesting a buildup of nitrous oxide; this byproduct is a known inhibitor of vitamin B12 metabolism that renders the vitamin inactive (Pema *et al*., 1998; Stockton *et al*., 2017), likely generating cellular B12 deficiencies. Vitamin B12, also known as cobalamin, is essential for a variety of metabolic pathways, such as 1-carbon metabolism and methionine metabolism. B12 has also been thoroughly studied for its thermodynamic stability as a biomolecule that can only be synthesized by microorganisms, yielding broad implications for origin of life studies (Eschenmoser, 2011). Despite its high demand by cells, B12 is often sparsely found in marine environments such as the ocean, where it is largely depleted in surface waters and only measurable in femtomolar to low picomolar concentrations (Menzel and Spaeth, 1962; Sanudo-Wilhelmy *et al*., 2012; Ellis *et al*., 2017). Supporting our conclusion that these cells were challenged by inhibition or depletion of vitamin B12, vitamin B transporters increased in abundance in all −5°C conditions (BtuB; Figs. 4 and 5A–D). The lack of intracellular vitamin B12, whether through a cellular inability to acquire or through inactivation via nitrous oxide, appears to cause a number of consequences in the cell.

Sulfate reduction was activated in all −5°C conditions compared to the control, demonstrating a cold-adapted sulfate metabolic response in *Cp*34H. Sulfate reduction has been previously noted to be more active in psychrophilic marine bacteria compared to warmer-adapted marine bacteria (Knoblauch *et al*., 1999a; Knoblauch *et al*., 1999b) and general carbon turnover rates in Arctic marine sediments are comparable to temperate climates due to their activity (Sageman *et al*., 1998). This, however, is the first analysis to reveal that sulfate reduction enzymes in a psychrophilic bacterium increased in response to lower subzero temperatures (i.e., −1°C to −5°C) regardless of nutrient input (CysC, CysJ, CysI, CysH, CysN, CysD, Fig. 5A–D; Dataset S9). *Cp*34H has been previously noted to have an enhanced genomic potential for sulfur metabolism, possessing both the ability to oxidize intracellular sulfur and acquire sulfur extracellularly through sulfatase production (Methé *et al*., 2005). Further, sulfur metabolism could be driven by the increase in cysteine and methionine metabolism experienced by cells in all conditions as a general response to a decrease in temperature. Complete activation of the methionine biosynthesis pathway was observed in all conditions (MetA, MetB, MetC, MetE, MetH, MetK, MetL, Figs. S13–S16; Dataset S9). Substitutions of various amino acids for methionine, previously observed to be increased in psychrophilic proteins, could stabilize the metal-binding domains of protein structures under low temperature conditions (Harvilla *et al*., 2014; De Maayer *et al*., 2014). Because the −5°C treatments were incubated for 4 months, increases in sulfate reduction may be a result of oxygen limitation. Calculations based on the growth rates tracked with [3H]-leucine

suggest that the oxygen is reduced by the end of the first week in the ASW^{+nutr} incubation (Table 1), further supporting the presence of anaerobic metabolic pathways being captured by the proteome at month four. These findings suggest that when overwintering, psychrophilic sulfate reducing enzymes can increase in abundance as temperatures drop, potentially influencing global sulfur cycles (Karr *et al*., 2005). Additionally, heterotrophic bacteria in anaerobic conditions of evolving glacial lakes also exhibit active sulfate reduction, suggesting these metabolic pathways may have increased relevance in other planetary lakes, such as on Titan (Rabus *et al*., 2004; Parro *et al*., 2016).

Survivable and detectable polypeptide biomarkers

These are the first incubations of *Cp*34H in supercooled ASW and equilibrium brine where activity, culturability and proteomics were simultaneously monitored. Based on previous work that indicates activity at −10°C in ice samples for extended periods of time (Junge *et al*., 2006; Nunn *et al*., 2015), visual evidence that our incubations maintained cell numbers at −10°C in all treatments, and results presented here that detected protein profiles at −10°C significantly differed from controls support the hypothesis that cells in extreme conditions on an icy world could retain specific polypeptide signatures for life at these conditions. This study represents the first statistical evaluation of detected bacterial peptide sequences to determine if short peptide motifs (3–4 amino acid long) were specifically synthesized and/or retained as a result of the high salinity or low −10°C temperature (Table S5). Evidence of the enrichment of short peptides in icy-world-analog incubations here on Earth provide environment-specific context for future discoveries of detectable biomarkers for life (extant or extinct) on other icy worlds. Currently, no multi-amino acid-based biomarkers for life exist, but here we provide a list of potential candidate polypeptides that could be targeted using high mass accuracy lander-based or in-orbit mass spectrometers (for review see Arevalo *et al*., 2020). Candidate biomarkers must be detectable by mass spectrometry and include polypeptide sequences of 2–8 amino acids in length; for statistical reasons, our analysis focuses on polypeptides of 3–4 amino acids in length.

The most extreme experimental condition, −10°C brine, representative of the response of terrestrial organisms to highly saline ice, especially under low-nutrient circumstances, is of distinct astrobiological relevance. Our analysis identified over 534 k-mers that were found to be significantly increased in *Cp*34H (Fig. S5; Dataset S10). These peptides are specifically enriched in the amino acids Ala, Val, Glu and Gln. Over 80 amino acids have been detected in carbonaceous meteorites (Pizzarello and Holmes, 2009; Pizzarello *et al*., 2006; Georgiou, 2018), and the most dominant alpha-amino acids discovered in meteorites follows a distribution of Gly > Ala > Glu > Asp > Ser (Davila and McKay, 2014), notably containing two of the dominant amino acids detected to be enriched in k-mers (Ala and Glu) at the more extreme conditions studied here (Table S5). Alanine is the second smallest of the 20 alpha-amino acids and is used in synthetic peptide design as a small spacer amino acid, providing non-charged flexibility (Walters and DeGrado, 2006 and citations within). The increased abundance of alanine in both 3- and 4-mers in both the temperature- and brine-specific enrichment analyses also suggests that alanine provides a flexible spacer to connect functional or acidic residues with higher binding affinities or catalytic propensities (Bartlett *et al*., 2002; Table S5). Valine, another frequently encountered amino acid in meteorites (Cobb and Pudritz, 2014), is noted to have a short hydrophilic side chain, providing valine-rich peptides with greater flexibility and activity at low temperatures.

Georgiou (2018) proposed that different combinations of amino acids generate specific catalytic units that may be enriched in life on earth, thereby increasing the probability of being discovered in primitive extraterrestrial life forms. Examinations of catalytic sites within enzymes suggest that two of the amino acids revealed to be enriched, retained, and detected in *Cp*34H k-mers have key chemical groups that can increase catalytic potential (Gln: amide, Glu: carboxylate; Bartlett *et al*., 2002). Previous analyses of > 190 catalytic enzymes' three-dimensional structures and functional sites identified six common catalytic triads (*Thr-His-His, Ser-His-Asp, Ser-His-Glu, Asp-Thr-Lys, Thr-Lys-Asp, Lys-Glu-Lys*; Gutteridge and Thornton, 2005). None of these 3-mers were identified in our analysis of enriched k-mers with the exception of *Ser-His-Asp* (SHD), a catalytic site of hydrolase serine proteases, identified in one temperature-specific 4-mer *Ser-His-Asp-Arg* (SHDR). The k-mer identified to be enriched in the temperature-, salinity- and brine-10°C- specific responses, *Lys-Asp-Ala* (KDA), is present in 189 of the predicted proteins from *Cp*34H. Although the sequence is short, it may enhance the functionality of these proteins in subzero temperatures as it has an acidic residue with a basic amide functional group (K), a carboxylate functional group (D), and a small non-polar spacer amino acid (A). In colder temperatures, where protein structures can become rigid and inflexible, the small amino acid spacer would provide a wider opening for other molecules to bind with adjacent catalytic amino acids.

Although individual amino acids have been detected in meteorites, and numerous models and predictions based on physical properties of known enzymes have been

made to theorize on novel life detection strategies, this report is the first to take detectable polypeptide biosignatures from psychrophiles incubated in extreme environmental conditions with the goal of identifying common, short, repeating patterns that might be found elsewhere in the Solar System. These peptides could be included in immunoassay-based life detector chips as proposed by Parro and colleagues (2016), or directly detected and verified using tandem mass spectrometry methods (e.g., Arevalo *et al*., 2020). Since peptides fragment in a predictable manner, generating a forward and backward conformational sequence fingerprint with b- and y-ions, high mass-accuracy mass spectrometry methods have a distinct advantage for detecting the proposed list of k-mers. Furthermore, for off-planet missions to detect life, mass spectrometers have flight heritage as they have been tested on missions to Mars dating back to the 1970s Viking mission (Anderson *et al*., 1972). Mass spectrometers can provide sensitive and quantitative analyses of the chemical composition of a range of planetary matrices, decipher isotopic, elemental and molecular abundances in an unbiased manner, and, with more recent advancements, allow for and direct complex experiments in the gas phase using tandem mass spectrometers, making them capable payload instruments for helping confidently detect biomarkers of life (e.g., Arevalo *et al*., 2019). For example, using tandem mass spectrometry, mission control will be able to design experiments that first accumulate predetermined ions (i.e., specific mass to charge ratios), while ejecting all other ions. This increases the signal to noise ratio, improves sample-specific detection limits, and yields higher resolution fragmentation spectra (i.e., MS2) for downstream interpretation. Mission-ready high mass-accuracy Orbitraps are already under development, showing great promise for detecting 3–4 amino acid long polypeptides (Arevalo *et al*., 2018). With known polypeptide targets, such as we provide here, pre-programmed parallel reaction monitoring mass spectrometry (PRM-MS) methods can be designed to target, isolate and fragment desired peptide masses of interest in the gas phase. The sensitivity of these MS based-methods have demonstrated detection of attomolar levels of many peptides within complex matrices (Gillette and Carr, 2013; Glukhova *et al*., 2013). Additionally, mass spectrometers would allow for on-the-fly organic or inorganic target selection from ground control so that these instruments can discover unexpected signals in a targeted-assay-like manner as new information is gained while in orbit.

The list of k-mers provided here reveals important trends in amino acid sequences and should be further refined as they are explored in other organisms. Although peptides have been subjectively placed low on the 'evidence for life' scale, directly correlating specific features that are enriched in terrigenous systems similar to those anticipated off-Earth may allow us to link heritable traits found as a molecular signal to specific environmental responses (Neveu *et al*., 2018). Direct correlations of k-mers featured here to high salinity or low temperature would strengthen evidence for the existence of life elsewhere if discovered off-planet. In addition to performing additional tests on these k-mers in other organisms, these peptides can be used in other low biomass, subzero or saline environments to determine their universality as a life detection biomarker. Isotopically-labelled synthetic duplicates should be made as laboratory standards and limits of quantification and detection should be established with mass spectrometry methods in a variety of matrices, including rock with potential relevance to the joint NASA and ESA future Mars rock and soil sample return campaign.

Concluding remarks

Conditions in the most extreme cold environments on Earth provide a useful analog to study other icy worlds, where survival would require organisms to maintain adaptations to extreme low temperatures and high salinities. Long-term survival in a matrix of extreme conditions can offer valuable clues to the metabolic strategies employed by microbial life-forms enduring similar combinations of stresses as the experimental variables explored in this study. Additionally, as specific proteins were uniquely identified and/or significantly increased or decreased in direct correlation to isolated variables, peptides from those proteins could be selected as biomarkers for extant life here and elsewhere.

Understanding the specific mechanisms by which extremophiles adapt to their surroundings is important for the progress of environmental, technological and astrobiological advancements. Here we report how environmental variables of low temperature, high salinity and absence of nutrients independently affect functional proteomic responses in the context of culturability and metabolic activity of *Cp*34H, particularly highlighting the impact of carbon, nitrogen and fatty acid metabolism. Finally, we propose the use of polypeptide biomarkers in advancing astrobiological searches for life on other icy worlds, providing a suitable list of candidate biomarkers to investigate in future studies.

Experimental procedures

Supercooled sea water and equilibrium brines

We prepared three sterile saline solutions (artificial seawater (ASW) at 6°C, equilibrium brine at −5°C and −10°C). The ionic composition of the solutions was

chosen to reflect the freezing-equilibrium concentrations of seawater at −1°C, −5°C and −10°C resulting in salinities of 35, 84 and 140 ppt with respective salt content of 3.5%, 8.4% and 14% (Table S1, Marion *et al*., 1999). Recipes for saline solutions were calculated to achieve the desired molal concentrations for each temperature (Table S2). Solutions were prepared with 1000 g of milli-Q water previously amended with 1.3 g/L of the buffer TAPSO (3-[N-tris(hydroxymethyl) methylamino]-2-hydroxypropane-sulfonic acid) and titrated to a pH of 7.6. Individual marine salts listed in Table S2 were added to the buffered milli-Q water at room temperature. Care was taken to prevent mineral precipitation at room temperature by mixing $CaCl_2$ separately in half of the water volume and slowly titrating the $CaCl_2$ solution into a solution containing the remaining salts. After preparation, saline solutions were filter-sterilized using 0.2 μm capfilters. Equilibrium ionic concentrations in Table S1 were converted to salt concentrations (%) following Marion and Kargel (2008). Water activity for brines was calculated based on the equilibrium constant of ice, a function of temperature (Spencer *et al*., 1990).

Bacterial strain and cellular preparations

Cell preparations were obtained from cultures of *C. psychrerythraea* strain 34H (ATCC No. BAA-681; GenBank Accession No. AF396670). *Cp*34H was cultured from frozen glycerol stocks, and then grown to early stationary phase in half-strength Marine Broth 2216 (SIGMA, Junge *et al*., 2006), rocking, at 0°C to a final cell density of 1.04×10^9 cells ml^{-1} (OD_{600} = 0.44).

The culture was split into three equal parts and centrifuged under sterile conditions at 2,800 × *g* for 20 min at 4°C (Nunn *et al*., 2015). After discarding the supernatant, cells were resuspended in either one of the three pre-chilled sterile saline solutions (see above), centrifuged again at 2,800 × *g* for 10 min at 4°C and resuspended in their corresponding pre-chilled saline solution for a final OD_{600} of 0.26 (ASW), 0.29 (−5°C brine) and 0.28 (−10°C brine). Triplicate 100 μl aliquots of cell resuspension were fixed in 2% formaldehyde and stored at 4°C for the determination of bacterial abundance through epifluorescence microscopy (see Culturability and cell abundance (cell counts)); another set of triplicate 20 μl aliquots was used to determine culturability through the most probable number (MPN) procedure as described below. The resulting initial cell concentrations were 3.12×10^8, 3.39×10^8 and 2.75×10^8 cells ml^{-1} for ASW, −5°C and −10°C brine respectively. The initial MPN of culturable cells were 2.15×10^8, 3.75×10^8 and 2.15×10^8 cells ml^{-1} for ASW, −5°C and −10°C brine respectively.

Cells resuspended in saline solutions were either used without further amendments (−nutr superscript) or amended with glucose (1 g/L), yeast extract (14 mg/L) and leucine (4 mg/L; +nutr superscript). Nutrient concentrations used here are known to support growth in *Cp*34H (Marx *et al*., 2009; Czajka *et al*., 2018). Cell resuspensions intended for activity measurements were amended with glucose and yeast extract only, as the radioactive marker already contained leucine. Parallel growth curves of *Cp*34H in ASW with and without nutrients at −1°C for 16 days were also performed to confirm that this minimal amount of nutrients can support growth and culturability under optimal temperature and salinity conditions (Dataset S2).

Incubations

Prior to incubation at the two temperatures, cell resuspensions were distributed into1.5 ml microcentrifuge tubes (Fisherbrand™ Premium) to be used for measurements of metabolic activity (500 μl cell resuspensions for protein synthesis through [3H]-leucine incorporation), measurements of cell abundance and culturability (600 μl cell resuspension, shared) and proteomics (600 μl cell resuspension). To determine protein synthesis activity, triplicate samples of both live incubations and killed control cells were retrieved at 2, 12, 24 h and 1 month. Metabolic activity incubations were completed at 1 month since previous studies had shown that subzero activity rates based on increases of leucine incorporations over time until maximum incorporation amounts are reached can usually be calculated during initial 24 h incubation periods, thus allowing for the determination of activity rates for the different treatments (Junge *et al*., 2006; Nunn *et al*., 2015). Samples for cell counts and cell culturability were retrieved after initial set-up and after 1 (n = 3) and 4 months (n = 4). Samples for proteomic analysis were harvested after 4 months (n = 4).

Microcentrifuge tubes were placed in plastic racks, wrapped in bubble wrap casings to reduce temperature fluctuations and transferred to −5°C and −10°C incubators. Fluctuations in incubator temperature were monitored prior to the start of the experiment, and the minimum temperature registered in a few days period was either −5°C or −10°C. Based on measured cooling rates, samples reached their target incubation temperature within 1 h.

To generate a reference proteomic dataset (control) from which all experimental proteomic datasets were compared, *Cp*34H was grown at −1°C and harvested at mid-exponential growth. Specifically, three cultures of *Cp*34H were grown in 20 ml of ½ × MB2216 (BD Difco) at −1°C, stirring, to a final cell density of $4.82 \times 10^8 \pm 3.18 \times 10^7$ cells ml^{-1}. Initial inocula were

derived from the same frozen glycerol stock used for all other cell resuspensions. From each flask, one 1 ml aliquot was obtained and killed with an immediate addition (i.e., within seconds) of 200 μl of pre-chilled 50% trichloroacetic acid (TCA). Any possible effect of opening the tube (and allowing more oxygen to enter for a few seconds) is considered negligible. Another 1 ml aliquot was fixed with 2% formaldehyde and stored at 4°C for analysis of microbial abundance. TCA-killed samples were centrifuged at 5000 × *g* for 20 min at 4°C, then washed with cold, sterile ASW and centrifuged again at 18,000 × *g* for 15 min at 4°C. Pellets were stored at −70°C until proteomic sample preparation (as described below).

Culturability and cell abundance (cell counts)

At each time point, each microcentrifuge tube was subsampled for culturability, cell abundance and proteomic analysis (Dataset S1). Culturability was determined by aliquoting 20 μl into triplicate wells of a pre-chilled 96-well microplate containing 180 μl of ½ × MB 2216. Ten serial 1:10 dilutions were performed on each triplicate sample. Microplates were incubated at 4°C until wells in the microplate showed visible turbidity. The number of wells displaying growth was converted into three-digit codes used to calculate the most probable number of culturable cells (MPN) according to standard tables from the FDA Bacteriological Analytical Manual (Blodget, 2011). To determine cell abundances, 100 μl aliquots were fixed in 2% formaldehyde and kept at 4°C until epifluorescence microscopy enumeration. Cells were stained with the DNA-fluorescent stain DAPI (4′,6′-diamidino-2-phenylindole 2HC) and microscopic counts were performed in triplicate as in Junge and colleagues (2004).

Metabolic activity: [3H]-leucine incorporation

Bacterial metabolic activity was measured using [3H]-leucine incorporation assays previously developed for the analysis of bacterial protein synthesis activity of *Cp*34H in saline ice (Junge *et al*., 2006; Nunn *et al*., 2015). Briefly, incubations for the metabolic activity assays contained 100 μl of the radioactive tracer ([3H]-leucine (10 Ci ml^{-1}; diluted 1:100 from stock of [3H]-leucine [ICN Biomedicals, Catalogue No. 20036E; 40–60 Ci ml^{-1} in sterile 2:98 ethanol–water mixture]). For controls, 100 μl of 50% chilled TCA were added to each microtube before tracer addition (as in Junge *et al*., 2006 and Nunn *et al*., 2015). Triplicate controls were completed at each temperature and time point. Methods described by Junge and colleagues (Junge *et al.,* 2006; Nunn *et al.,* 2015) were primarily followed, with the exception of one modification where two ethanol washes were performed during the processing stage.

Proteomic sample preparations

After 4 months of incubation, a 440 μl aliquot from each 600 μl cell suspension sample was subsampled, killed with 88 μl of cold 50% TCA, and cell debris and proteins were pelleted at 18,000 × *g* for 15 min at 4°C. After discarding supernatant, pellets were frozen at −70°C until proteomic sample preparation. All TCA-precipitated cell pellets for proteomic analyses were mechanically lysed (Branson 250 Sonifier; 20 kHz, 10 × 10 s on ice) and then proteins were solubilized, quantified and digested following the detailed methods outlined in Nunn and colleagues (2015). Briefly, 100 μg aliquots of protein were reduced (tris(2-carboxyethyl)phosphine (TCEP), alkylated (iodoacetamide) and then digested with Promega modified trypsin (4 h 37°C). Peptides were desalted using C18 miniprep centrifugal spin columns following manufacturer's instructions (Nest group MicroSpin columns) and cleaned up peptides were evaporated to dryness and resuspended in 2% acetonitrile (ACN), 0.1% formic acid with final concentration of 0.5 μg protein μl^{-1}.

Proteomic mass spectrometry

The mass spectrometry analysis was performed on a QExactive Hybrid Quadrupole Orbitrap with an inline EASY-nLC 1200 (ThermoFisher Scientific). Reverse-phase chromatography was achieved using a Manufactured PicoTip fused silica capillary column (40 cm long, 75 μm i.d.) packed in-house with C18 particles (Dr. Maisch ReproSil-Pur; C18-Aq, 120 Å, 3 μm) fitted with an in-house packed kasil-frit 3 cm long, 100 μm i.d. precolumn (Dr. Maisch ReproSil-Pur; C18-Aq, 120 Å, 3 μm). To maintain a stable back-pressure on the liquid chromatography column, the 40 cm analytical column was held at 40°C. Peptides were eluted using an acidified (formic acid, 0.1% v/v) water-acetonitrile gradient (2%–35% acetonitrile in 120 min). The top 20 most intense ions were selected for MS2 acquisition from precursor ion scans of 400–1200 *m/z*. Centroid full MS resolution data was collected at 70,000 with AGC target of 1×10^6 and centroid MS2 data was collected at resolution of 35,000 with AGC target of 5×10^4. Dynamic exclusion was set to 10 s and +2, +3, +4 ions were selected for MS2 using data dependent acquisition mode (DDA). Sample analyses on the MS were randomized to reduce batch effects and quality control (QC) peptide mixtures were analysed every fifth injection to monitor chromatography and MS sensitivity. Skyline was used to determine that QC standards did not deviate > 10% through all analyses (MacLean *et al*., 2010). The mass spectrometry

data are deposited to the Proteome Xchange Consortium via the PRIDE partner repository with the dataset identifier PXD022428 (username: reviewer_pxd022428@ebi.ac.uk; password: UoNMy87v).

Protein data interpretation

Peptide identifications from mass spectrometry data were completed using Comet 2018.01 rev. 2 (Eng *et al*., 2013, 2015) and the Uniprot *C. psychrerythraea* protein database (downloaded 4/2/2019) concatenated with 50 common contaminants and the QC peptides. Comet parameters included: reverse concatenated sequence database search, trypsin enzyme specificity, cysteine modification of 57 Da and modifications on methionine of 15.999 Da (oxidation). PeptideProphet and ProteinProphet were used to validate peptide spectral matches (PSMs) and determine thresholds for a false discovery rate < 0.01 (proteins accepted if ≥ 2 peptides identified, and $P > 0.95$ on ProteinProphet and $P > 0.99$ on PeptideProphet (Nesvizhskii *et al*., 2003). Abacus (in the QPROT software suite) was used to generate normalized spectral abundance factors (NSAF), the number of unique peptides identified for each protein across all experiments, and PSM counts for all confidently identified proteins (Fermin *et al*., 2011; Choi *et al*., 2015; Dataset S4). NSAF corrects for the effect of protein length on final spectral counts, as larger proteins inherently contribute more peptides. NSAF is calculated as the number of spectral counts for a protein (SpecCnt), divided by the protein length (L; i.e., the number of amino acids), divided by the sum of SpecCnt/L for all proteins identified in a mass spectrometry experiment. NSAF values were further analysed with QPROT to determine pairwise $\log_2$ fold changes between treatments and were plotted using ggplot2 to generate volcano plots (Choi *et al*., 2015; Wickham, 2016; Dataset S9). All data presented to be significantly changing passed $\log_2$ fold-change ≥ |0.5| and Z-statistic score ≥ |2.0| (equivalent to P-value < 0.05; two tailed; Choi *et al*., 2015). Nonparametric multidimensional scaling analysis (NMDS) was completed on NSAF values for each bioreplicate with ≥ 2 unique peptides identified per treatment using the package 'vegan' with R studio version 1.2.1335 (Oksanen *et al*., 2013, 2019; Rstudio Team, 2020; Dataset S4, Dataset S5). Hierarchical clustering analysis was completed using the package 'pheatmap' on peptides meeting more stringent significance thresholds of $\log_2$ fold-change ≥ |2| and Z-statistic score ≥ |2.0| (Dataset S7) (Kolde, 2019). Upset plots and venn diagrams were completed on datasets where ≥ 2 unique peptides were detected across all experiments, and ≥ 2 spectral counts per bioreplicate (Chen, 2018; Gehlenborg, 2019; Dataset S6). A defined list of 21 functional annotation terms for categorizing proteins was selected using EggNOG-mapper version 5.0, a database for defining proteins using orthologous relationships and gene evolutionary histories (Huerta-Cepas *et al*., 2019; Dataset S8). All identified proteins were also annotated with Kyoto Encyclopaedia of Genes and Genomes (KEGG) using KOALA (Kanehisa *et al*., 2016), assigning K numbers to identified metabolic enzymes (Dataset S9). Proteins identified to be significantly changing were mapped onto pre-existing metabolic maps using KEGG Mapper – Search & Colour Pathway tool (https://www.genome.jp/kegg/tool/map_pathway2.html).

Enrichment analysis of salinity and temperature-specific short polypeptides

Enrichment analyses of the amino acid sequences retained after 4 months at −10°C were completed to determine if there were short peptide sequences (3–4 amino acids) that were significantly enriched relative to the short peptide sequences from all of the proteins detected across these experiments. Peptide-spectrum matches (PSMs) were post-processed using Percolator (Käll *et al*., 2007) to detect peptides in each run at a false discovery rate (FDR) threshold of 1%. NSAF values from all MS experiments on the four treatment conditions were analysed using two-factor analysis of variance (ANOVA) with 1% FDR control via the Benjamini–Hochberg (BH) procedure to detect proteins associated with changes in temperature and salinity (Dataset S10). This analysis provided sets of proteins associated with temperature (−5°C vs. −10°C), salinity (ASW vs. equilibrium brines), and the interaction of the two terms (all conditions vs. −10°C brine treatments). From the proteins identified in the ANOVA, $\log_2$ fold change was computed followed by a one-tailed t-test (with BH FDR control at 1%) to determine significantly changing proteins between different treatments ($\log_2$ fold change ≥0.5). Proteins identified to be significantly different in response to high salinity, −10°C temperatures, or the combined effects in the −10°C brines were then digested *in silico* to 3–4 amino acid long k-mers, and statistically evaluated relative to the background lists of 3-mers and 4-mers detected across all experiments to identify condition-specific enriched short polypeptides. A chi-squared test was performed on the k-mer counts in each condition, with BH multiple testing correction, providing a q-value and $\log_2$ fold change value for each k-mer and allowing identification of statistically different frequencies of the k-mers observed in the different treatments (Dataset S10). A second chi-squared test was performed to determine which, if any, amino acid compositions of the identified 3-mers and 4-mers were significantly increased or decreased relative to the amino acid distribution of all

detected peptide k-mers. Heatmaps were generated to visualize the distribution of amino acids in the 3-mers and 4-mers, irrespective of the location in the sequence, where rows representing amino acid distributions were clustered using Euclidean distances. Principal component analysis was completed using Python using scikit-learn package v.0.21.3, and all code and scripts are provided in the Github repository github.com/noble-lab/2020_cp34h.

Acknowledgements

This work was supported by funding from a grant awarded by the NASA Exobiology program to K. Junge and B.L. Nunn, B. Light and J. Toner (grant number 80NSSC18K1291). M.C. Mudge and W.E. Fondrie were supported by The Genome Science Training Grant (5T32HG000035-25) and W.S. Noble was funded by NIH R01 (R01GM121818). Experimental design, cell cultures and the activity and culturability data collection and analyses were completed by Junge, Ewert and Firth. Proteomic mass spectrometry, including sample preparations and all proteomic data analyses, including biomarker identifications, were completed by Mudge and Nunn. The enrichment analyses of k-mer biomarkers for life detection were completed by Fondrie, Hales, Noble and Nunn. This work is supported in part by the University of Washington's Proteomics Resource (UWPR95794). We thank Shelly Carpenter for performing cell counts and Izabela Carpenter who prepared the cell cultures for the proteomics controls. We thank Emma Timmins-Schiffman for participating in technical editing of the manuscript.

References

Akhtar, N., Karabika, E., Kinghorn, J.R., Glass, A.D.M., Unkles, S.E., and Rouch, D.A. (2015) High-affinity nitrate/nitrite transporters NrtA and NrtB of *Aspergillus nidulans* exhibit high specificity and different inhibitor sensitivity. *Microbiology* **161**: 1435–1446.

Akhtar, S., Khan, A., Sohaskey, C.D., Jagannath, C., and Sarkar, D. (2013) Nitrite Reductase NirBD is induced and plays an important role during in vitro dormancy of *Mycobacterium tuberculosis*. *J Bacteriol* **195**: 4592–4599.

Anderson, D.M., Biemann, K., Orgel, L.E., Oro, J., Owen, T., Shulman, G.P., *et al*. (1972) Mass spectrometric analysis of organic compounds, water and volatile constituents in the atmosphere and surface of Mars: the Viking Mars Lander. *Icarus* **16**: 111–138.

Andreesen, J.R. (1994) Glycine metabolism in anaerobes. *Antonie Van Leeuwenhoek* **66**: 223–237.

Ardyna, M., and Arrigo, K.R. (2020) Phytoplankton dynamics in a changing Arctic Ocean. *Nat Climate Change* **10**: 892–903.

Arevalo, R., Ni, Z., and Danell, R.M. (2020) Mass spectrometry and planetary exploration: a brief review and future projection. *J Mass Spectrom* **55**: 4454.

Arevalo, R., Selliez, L., Briois, C., Carrasco, N., Thirkell, L., Cherville, B., *et al*. (2018) An Orbitrap-based laser desorption/ablation mass spectrometer designed for spaceflight. *Rapid Commun Mass Spectrom* **32**: 1875–1886.

Arevalo, Jr, R., Southard, A.E., Grubisic, A., Danell, R., Gundersen, C., and Minasola, N.A. (2019) CORALS: Characterization of Ocean Realms and Life Signatures. *AGU Fall Meeting Abstracts* **1**: P34C–04.

Ayrapetyan, M., and Oliver, J.D. (2016) The viable but non-culturable state and its relevance in food safety. *Curr Opin Food Sci* **8**: 127–133.

Baker, J.M., Riester, C.J., Skinner, B.M., Newell, A.W., Swingley, W.D., Madigan, M.T., *et al*. (2017) Genome sequence of *Rhodoferax antarcticus* ANT.BRT; a psychrophilic purple nonsulfur bacterium from an Antarctic microbial mat. *Microorganisms* **5**: 8.

Bartlett, G.J., Porter, C.T., Borkakoti, N., and Thornton, J.M. (2002) Analysis of catalytic residues in enzyme active sites. *J Mol Biol* **324**: 105–121.

Bianco, C.M., Fröhlich, K.S., and Vanderpool, C.K. (2019) Bacterial cyclopropane fatty acid synthase mRNA is targeted by activating and repressing small RNAs. *J Bacteriol* **201**: e00461-19.

Blodget, R. (2011) Bacteriological Analytical Manual, Dataset 2, Most Probable Number from Serial Dilutions. FDA.

Boetius, A., Anesio, A.M., Deming, J.W., Mikucki, J.A., and Rapp, J.Z. (2015) Microbial ecology of the cryosphere: sea ice and glacial habitats. *Nat Rev Microbiol* **13**: 677–690.

Bolam, D.N., and van den Berg, B. (2018) TonB-dependent transport by the gut microbiota: novel aspects of an old problem. *Curr Opin Struct Biol* **51**: 35–43.

Bowman, J.P. (2017) Genomics of psychrophilic bacteria and archaea. In *Psychrophiles: From Biodiversity to Biotechnology*, Margesin, R. (ed). Cham: Springer International Publishing, pp. 345–387.

Bowman, J.P., Gosink, J.J., McCammon, S.A., Lewis, T.E., Nichols, D.S., Nichols, P.D., *et al*. (1998) *Colwellia demingiae* sp. nov., *Colwellia hornerae* sp. nov., *Colwellia rossensis* sp. nov. and *Colwellia psychrotropica* sp. nov.: psychrophilic Antarctic species with the ability to synthesize docosahexaenoic acid (22:ω63). *Int J System Evol Microbiol* **48**: 1171–1180.

Carr, M.H., Belton, M.J.S., Chapman, C.R., Davies, M.E., Geissler, P., Greenberg, R., *et al*. (1998) Evidence for a subsurface ocean on Europa. *Nature* **391**: 363–365.

Castillo-Keller, M., Vuong, P., and Misra, R. (2006) Novel mechanism of *Escherichia coli* porin regulation. *J Bacteriol* **188**: 576–586.

Cezairliyan, B., and Ausubel, F.M. (2017) Investment in secreted enzymes during nutrient-limited growth is utility dependent. *Proc Natl Acad Sci U S A* **114**: E7796–E7802.

Chattopadhyay, M.K. (2006) Mechanism of bacterial adaptation to low temperature. *J Biosci* **31**: 157–165.

Chen, H. (2018) VennDiagram: Generate High-Resolution Venn and Euler Plots. R package version 1.6.20. URL https://CRAN.R-project.org/package=VennDiagram.

Chen, Y., and Wang, F. (2015) Insights on nitrate respiration by Shewanella. *Front Mar Sci* **1**: 1–9.

Choi, H., Kim, S., Fermin, D., Tsou, C.-C., and Nesvizhskii, A.I. (2015) QPROT: statistical method for testing differential expression using protein-level intensity data in label-free quantitative proteomics. *J Proteomics* **129**: 121–126.

Choi, U., and Lee, C.-R. (2019) Distinct roles of outer membrane Porins in antibiotic resistance and membrane integrity in *Escherichia coli*. *Front Microbiol* **10**(953): 1–9.

Clark, S.C., Granger, J., Mastorakis, A., Aguilar-Islas, A., and Hastings, M.G. (2020) An investigation into the origin of nitrate in Arctic Sea ice. *Global Biogeochem Cycles* **34**: e2019GB006279.

Cobb, A.K., and Pudritz, R.E. (2014) Nature's starships. I. Observed abundances and relative frequencies of amino acids in meteorites. *Astrophysics* **783**: 140.

Collins, R.E. (2009) Microbial Evolution In Sea Ice: Communities To Genes. Thesis.

Collins, R.E., Carpenter, S.D., and Deming, J.W. (2008) Spatial heterogeneity and temporal dynamics of particles, bacteria, and pEPS in Arctic winter sea ice. *J Mar Syst* **74**: 902–917.

Collins, R.E., and Deming, J.W. (2013) An inter-order horizontal gene transfer event enables the catabolism of compatible solutes by *Colwellia psychrerythraea* 34H. *Extremophiles* **17**: 601–610.

Cox, G.F.N., and Weeks, W.F. (1983) Equations for determining the gas and brine volumes in sea-ice samples. *J Glaciol* **29**: 306–316.

Cox, G.F.N., and Weeks, W.F. (1986) Changes in the salinity and porosity of sea-ice samples during shipping and storage. *J Glaciol* **32**: 112.

Craig, L., Forest, K.T., and Maier, B. (2019) Type IV pili: dynamics, biophysics and functional consequences. *Nat Rev Microbiol* **17**: 429–440.

Creamean, J.M., Cross, J.N., Pickart, R., McRaven, L., Lin, P., Pacini, A., *et al*. (2019) Ice nucleating particles carried from below a phytoplankton bloom to the Arctic atmosphere. *Geophys Res Lett* **46**: 8572–8581.

Czajka, J.J., Abernathy, M.H., Benites, V.T., Baidoo, E.E.K., Deming, J.W., and Tang, Y.J. (2018) Model metabolic strategy for heterotrophic bacteria in the cold ocean based on *Colwellia psychrerythraea* 34H. *Proc Natl Acad Sci U S A* **115**: 12507–12512.

Davila, A.F., and McKay, C.P. (2014) Chance and necessity in biochemistry: implications for the search for extraterrestrial biomarkers in earth-like environments. *Astrobiology* **14**: 534–540.

De Maayer, P., Anderson, D., Cary, C., and Cowan, D.A. (2014) Some like it cold: understanding the survival strategies of psychrophiles. *EMBO Rep* **15**: 508–517.

Deming, J.W., and Young, J.N. (2017) The role of exopolysaccharides in microbial adaptation to cold habitats. In *Psychrophiles: From Biodiversity to Biotechnology*, Margesin, R. (ed). Cham: Springer International Publishing, pp. 259–284.

Denby, K.J., Iwig, J., Bisson, C., Westwood, J., Rolfe, M.D., Sedelnikova, S.E., *et al*. (2016) The mechanism of a formaldehyde-sensing transcriptional regulator. *Sci Rep* **6**: 38879.

Deng, Y., Chen, C., Zhao, Z., Zhao, J., Jacq, A., Huang, X., and Yang, Y. (2016) The RNA chaperone Hfq is involved in Colony morphology, nutrient utilization and oxidative and envelope stress response in *Vibrio alginolyticus*. *PLoS One* **11**: 1–15.

Dickson, J.L., Head, J.W., Levy, J.S., and Marchant, D.R. (2013) Don Juan pond, Antarctica: near-surface CaCl2 -brine feeding Earth's most saline lake and implications for Mars. *Sci Rep* **3**: 1166.

Eicken, H., and Salganek, M. (2009) *Field Techniques for Sea-Ice Research*. Fairbanks, AK: University of Alaska Press.

Ellis, K.A., Cohen, N.R., Moreno, C., and Marchetti, A. (2017) Cobalamin-independent methionine synthase distribution and influence on vitamin B12 growth requirements in marine diatoms. *Protist* **168**: 32–47.

Eng, J.K., Hoopmann, M.R., Jahan, T.A., Egertson, J.D., Noble, W.S., and MacCoss, M.J. (2015) A deeper look into comet—implementation and features. *J Am Soc Mass Spectrom* **26**: 1865–1874.

Eng, J.K., Jahan, T.A., and Hoopmann, M.R. (2013) Comet: an open-source MS/MS sequence database search tool. *Proteomics* **13**: 22–24.

Eschenmoser, A. (2011) Etiology of potentially primordial biomolecular structures: from vitamin B12 to the nucleic acids and an inquiry into the chemistry of life's origin: a retrospective. *Angew Chem Int Ed* **50**: 12412–12472.

Ewert, M., Carpenter, S.D., Colangelo-Lillis, J., and Deming, J.W. (2013) Bacterial and extracellular polysaccharide content of brine-wetted snow over Arctic winter first-year sea ice. *J Geophys Res Oceans* **118**: 726–735.

Ewert, M., and Deming, J.W. (2011) Selective retention in saline ice of extracellular polysaccharides produced by the cold-adapted marine bacterium *Colwellia psychrerythraea* strain 34H. *Ann Glaciol* **52**: 111–117.

Ewert, M., and Deming, J.W. (2014) Bacterial responses to fluctuations and extremes in temperature and brine salinity at the surface of Arctic winter sea ice. *FEMS Microbiol Ecol* **89**: 476–489.

Falb, M., Müller, K., Königsmaier, L., Oberwinkler, T., Horn, P., von Gronau, S., *et al*. (2008) Metabolism of halophilic archaea. *Extremophiles* **12**: 177–196.

Ferenci, T. (2005) Maintaining a healthy SPANC balance through regulatory and mutational adaptation. *Mol Microbiol* **57**: 1–8.

Fermin, D., Basrur, V., Yocum, A.K., and Nesvizhskii, A.I. (2011) Abacus: a computational tool for extracting and pre-processing spectral count data for label-free quantitative proteomic analysis. *Proteomics* **11**: 1340–1345.

Firth, E., Carpenter, S.D., Sørensen, H.L., Collins, R.E., and Deming, J.W. (2016) Bacterial use of choline to tolerate salinity shifts in sea-ice brines. *Elem Sci Anth* **4**: 000120.

Flamholz, A., Noor, E., Bar-Even, A., Liebermeister, W., and Milo, R. (2013) Glycolytic strategy as a tradeoff between energy yield and protein cost. *Proc Natl Acad Sci U S A* **110**: 10039–10044.

Fujita, M., Mori, K., Hara, H., Hishiyama, S., Kamimura, N., and Masai, E. (2019) A TonB-dependent receptor constitutes the outer membrane transport system for a lignin-derived aromatic compound. *Commun Biol* **2**: 1–10.

Fujita, Y., Matsuoka, H., and Hirooka, K. (2007) Regulation of fatty acid metabolism in bacteria. *Mol Microbiol* **66**: 829–839.

Geesey, G.G., and Morita, R.Y. (1979) Capture of arginine at low concentrations by a marine psychrophilic bacterium. *Appl Environ Microbiol* **38**: 1092–1097.

Gehlenborg, N. (2019) UpSetR: A More Scalable Alternative to Venn and Euler Diagrams for Visualizing Intersecting

Sets. R package version 1.4.0. URL https://CRAN.R-project.org/package=UpSetR.

Georgiou, C.D. (2018) Functional properties of amino acid side chains as biomarkers of extraterrestrial life. *Astrobiology* **18**: 1479–1496.

Gillette, M.A., and Carr, S.A. (2013) Quantitative analysis of peptides and proteins in biomedicine by targeted mass spectrometry. *Nat Methods* **10**: 28–34.

Glukhova, V.A., Tomazela, D.M., Findlay, G.D., Monnat, R. J., and MacCoss, M.J. (2013) Rapid assessment of RNAi-mediated protein depletion by selected reaction monitoring mass spectrometry. *J Proteome Res* **12**: 3246–3254.

Gold, V.A., Salzer, R., Averhoff, B., and Kühlbrandt, W. (2015) Structure of a type IV pilus machinery in the open and closed state. *Elife* **4**: e07380.

Golden, K.M., Eicken, H., Heaton, A.L., Miner, J., Pringle, D. J., and Zhu, J. (2007) Thermal evolution of permeability and microstructure in sea ice. *Geophys Res Lett* **34**: 1–6.

Gunde-Cimerman, N., Plemenitaš, A., and Oren, A. (2018) Strategies of adaptation of microorganisms of the three domains of life to high salt concentrations. *FEMS Microbiol Rev* **42**: 353–375.

Gutteridge, A., and Thornton, J.M. (2005) Understanding nature's catalytic toolkit. *Trends Biochem Sci* **30**: 622–629.

Hand, K.P., Chyba, C.F., Priscu, J.C., Carlson, R.W., and Nealson, K.H. (2009) Astrobiology and the potential for life on Europa. *Europa*. The University of Arizona space science series. Tuscon, AZ: University of Arizona Press, pp. 589–629.

Hand, K.P., Murray, A.E., Garvin, J.B., Brinckerhoff, W.B., Christner, B.C, Edgett, K.S, *et al*. (2017) Report of the Europa Lander Science Definition Team.

Harvilla, P.B., Wolcott, H.N., and Magyar, J.S. (2014) The structure of ferricytochrome c 552 from the psychrophilic marine bacterium *Colwellia psychrerythraea* 34H. *Metallomics* **6**: 1126–1130.

Hendrix, A.R., Hurford, T.A., Barge, L.M., Bland, M.T., Bowman, J.S., and Brinckerhoff, W. (2018) The NASA Roadmap to Ocean Worlds. *Astrobiology* **19**: 1–27.

Henley, S.F., Porter, M., Hobbs, L., Braun, J., Guillaume-Castel, R., Venables, E.J., *et al*. (2020) Nitrate supply and uptake in the Atlantic Arctic Sea ice zone: seasonal cycle, mechanisms and drivers. *Philos Trans R Soc A Math Phys Eng Sci* **378**: 20190361.

Huber, M., Fröhlich, K.S., Radmer, J., and Papenfort, K. (2020) Switching fatty acid metabolism by an RNA-controlled feed forward loop. *PNAS* **117**: 8044–8054.

Huerta-Cepas, J., Szklarczyk, D., Heller, D., Hernández-Plaza, A., Forslund, S.K., Cook, H., *et al*. (2019) eggNOG 5.0: a hierarchical, functionally and phylogenetically annotated orthology resource based on 5090 organisms and 2502 viruses. *Nucleic Acids Res* **47**: D309–D314.

Huston, A.L.. (2004) Bacterial adaptation to the cold: In situ activities of extracellular enzymes in the North Water Polynya and characterization of a cold-active aminopeptidase from Colwellia psychrerythraea strain 34H.

Huston, A.L., Krieger-Brockett, B.B., and Deming, J.W. (2000) Remarkably low temperature optima for extracellular enzyme activity from Arctic bacteria and sea ice. *Environ Microbiol* **2**: 383–388.

Ito, K., and Akiyama, Y. (2005) Cellular functions, mechanism of action, and regulation of FtsH protease. *Annu Rev Microbiol* **59**: 211–231.

Jackson, R.H., Cornish-Bowden, A., and Cole, J.A. (1981) Prosthetic groups of the NADH-dependent nitrite reductase from *Escherichia coli* K12. *Biochem J* **193**: 861–867.

Junge, K., Cameron, K., and Nunn, B. (2019) Chapter 12 - diversity of psychrophilic bacteria in sea and glacier ice environments—insights through genomics, Metagenomics, and proteomics approaches. In *Microbial Diversity in the Genomic Era*. Das, S., and Dash, H.R. (eds). Cambridge, MA: Academic Press, pp. 197–216.

Junge, K., Eicken, H., and Deming, J.W. (2003) Motility of *Colwellia psychrerythraea* strain 34H at subzero temperatures. *Appl Environ Microbiol* **69**: 4282–4284.

Junge, K., Eicken, H., and Deming, J.W. (2004) Bacterial activity at −2 to −20°C in Arctic wintertime sea ice. *Applied and Environ Microbiol* **70**(1): 550–557.

Junge, K., Eicken, H., Swanson, B.D., and Deming, J.W. (2006) Bacterial incorporation of leucine into protein down to −20 degrees C with evidence for potential activity in sub-eutectic saline ice formations. *Cryobiology* **52**: 417–429.

Käll, L., Canterbury, J.D., Weston, J., Noble, W.S., and MacCoss, M.J. (2007) Semi-supervised learning for peptide identification from shotgun proteomics datasets. *Nat Methods* **11**: 923–925.

Kanehisa, M., Sato, Y., and Morishima, K. (2016) BlastKOALA and GhostKOALA: KEGG tools for functional characterization of genome and metagenome sequences. *J Mol Biol* **428**: 726–731.

Karr, E.A., Sattley, W.M., Rice, M.R., Jung, D.O., Madigan, M.T., and Achenbach, L.A. (2005) Diversity and distribution of sulfate-reducing bacteria in permanently frozen Lake Fryxell, McMurdo dry valleys, Antarctica. *Appl Environ Microbiol* **71**: 6353–6359.

Katsaros, K. (1973) Supercooling at the surface of an Arctic lead. *J Phys Oceanogr* **3**: 482–486.

Khurana, K.K., Kivelson, M.G., Stevenson, D.J., Schubert, G., Russell, C.T., Walker, R.J., and Polanskey, C. (1998) Induced magnetic fields as evidence for subsurface oceans in Europa and Callisto. *Nature* **395**: 777–780.

Knoblauch, C., Jørgensen, B.B., and Harder, J. (1999a) Community size and metabolic rates of psychrophilic sulfate-reducing bacteria in Arctic marine sediments. *Appl Environ Microbiol* **65**: 4230–4233.

Knoblauch, C., Sahm, K., and Jørgensen, B.B. (1999b) Psychrophilic sulfate-reducing bacteria isolated from permanently cold Arctic marine sediments: description of *Desulfofrigus oceanense* gen. Nov., sp. nov., *Desulfofrigus fragile* sp. nov., *Desulfofaba gelida* gen. Nov., sp. nov., *Desulfotalea psychrophila* gen. nov., sp. nov. and *Desulfotalea arctica* sp. nov. *Int J Syst Evol Microbiol* **49**: 1631–1643.

Kolde, R. (2019). pheatmap: Pretty Heatmaps. R package version 1.0.12. URL https://CRAN.R-project.org/package=pheatmap.

Krembs, C., and Deming, J.W. (2008) The role of exopolymers in microbial adaptation to sea ice. In *Psychrophiles: From Biodiversity to Biotechnology*,

Margesin, R., Schinner, F., Marx, J.-C., and Gerday, C. (eds). Berlin, Heidelberg: Springer, pp. 247–264.

Krembs, C., Eicken, H., and Deming, J.W. (2011) Exopolymer alteration of physical properties of sea ice and implications for ice habitability and biogeochemistry in a warmer Arctic. *PNAS* **108**: 3653–3658.

Krembs, C., Eicken, H., Junge, K., and Deming, J.W. (2002) High concentrations of exopolymeric substances in Arctic winter sea ice: implications for the polar ocean carbon cycle and cryoprotection of diatoms. *Deep-Sea Res I Oceanogr Res Pap* **49**: 2163–2181.

Kuan, Y.-J., Huang, H.-C., Charnley, S.B., Markwick, A., Botta, O., Ehrenfreund, P., *et al*. (2003) Interstellar Organic Molecules: from Clouds to Solar Nebula 14.

Lauro, S.E., Pettinelli, E., Caprarelli, G., Guallini, L., Rossi, A.P., Mattei, E., *et al*. (2020) Multiple subglacial water bodies below the south pole of Mars unveiled by new MARSIS data. *Nat Astronomy* **5**: 1–8.

Lee, S.J., Jeong, E.M., Ki, A.Y., Oh, K.S., Kwon, J., and Jeong, J.H. (2016) Oxidative defense metabolites induced by salinity stress in roots of Salicornia herbacea. *J Plant Physiol* **206**: 133–142.

Li, X.-Z., and Nikaido, H. (2009) Efflux-mediated drug resistance in bacteria: an update. *Drugs* **69**: 1555–1623.

Liu, G., Cai, S., Hou, J., Zhao, D., Han, J., Zhou, J., and Xiang, H. (2016) Enoyl-CoA hydratase mediates polyhydroxyalkanoate mobilization in *Haloferax mediterranei*. *Sci Rep* **6**: 24015.

MacLean, B., Tomazela, D.M., Shulman, N., Chambers, M., Finney, G.L., and Frewen, B. (2010) Skyline: an open source document editor for creating and analyzing targeted proteomics experiments. *Bioinformatics* **26**(7): 966–968.

Marion, G.M., Farren, R.E., and Komrowski, A.J. (1999) Alternative pathways for seawater freezing. *Cold Reg Sci Technol* **29**: 259–266.

Marion, G.M., and Kargel, J.S. (2008) *Cold Aqueous Planetary Geochemistry with FREZCHEM: From Modeling to the Search for Life at the Limits*. Berlin, Heidelberg: Springer Berlin Heidelberg.

Martin, A., and McMinn, A. (2018) Sea ice, extremophiles and life on extra-terrestrial ocean worlds. *Int J Astrobiol* **17**: 1–16.

Martin, K.P., MacKenzie, S.M., Barnes, J.W., and Ytreberg, F.M. (2019) Protein stability in Titan's subsurface water Ocean. *Astrobiology* **20**: 190–198.

Marx, J.G., Carpenter, S.D., and Deming, J.W. (2009) Production of cryoprotectant extracellular polysaccharide substances (EPS) by the marine psychrophilic bacterium *Colwellia psychrerythraea* strain 34H under extreme conditions. *Can J Microbiol* **55**: 63–72.

McGeoch, M.W., Dikler, S., and McGeoch, J.E.M. (2020) Hemolithin: a Meteoritic Protein containing Iron and Lithium. Astrophysics ArXiv:2002.11688.

McKay, D.S., Gibson, E.K., Thomas-Keprta, K.L., Vali, H., Romanek, C.S., Clemett, S.J., *et al*. (1996) Search for past life on Mars: possible relic biogenic activity in Martian meteorite ALH84001. *Science* **273**: 924–930.

Meganathan, R. (2001) Ubiquinone biosynthesis in microorganisms. *FEMS Microbiol Lett* **203**: 131–139.

Menzel, D.W., and Spaeth, J.P. (1962) Occurrence of vitamin B12 in the Sargasso Sea. *Limnol Oceanogr* **7**: 151–154.

Methé, B.A., Nelson, K.E., Deming, J.W., Momen, B., Melamud, E., Zhang, X., *et al*. (2005) The psychrophilic lifestyle as revealed by the genome sequence of *Colwellia psychrerythraea* 34H through genomic and proteomic analyses. *PNAS* **102**: 10913–10918.

Mikan, M.P., Harvey, H.R., Timmins-Schiffman, E., Riffle, M., May, D.H., Salter, I., *et al*. (2020) Metaproteomics reveal that rapid perturbations in organic matter prioritize functional restructuring over taxonomy in western Arctic Ocean microbiomes. *ISME J* **14**: 39–52.

Mordukhova, E.A., and Pan, J.-G. (2013) Evolved Cobalamin-independent methionine synthase (MetE) improves the acetate and thermal tolerance of *Escherichia coli*. *Appl Environ Microbiol* **79**: 7905–7915.

Moyer, C.L., Eric Collins, R., and Morita, R.Y. (2017) Psychrophiles and Psychrotrophs. In *Reference Module in Life Sciences*. Amsterdam, Netherlands: Elsevier, B9780128096338022000.

Murray, A.E., Kenig, F., Fritsen, C.H., McKay, C.P., Cawley, K.M., and Edwards, R. (2012) Microbial life at −13°C in the brine of an ice-sealed Antarctic lake. *Proc Natl Acad Sci USA* **109**: 20626.

Nagore, D., Sanz, B., Soria, J., Llarena, M., Llama, M.J., Calvete, J.J., and Serra, J.L. (2006) The nitrate/nitrite ABC transporter of *Phormidium laminosum*: phosphorylation state of NrtA is not involved in its substrate binding activity. *Biochim Biophys Acta Gen Sub* **1760**: 172–181.

Nesvizhskii, A.I., Keller, A., Kolker, E., and Aebersold, R. (2003) A statistical model for identifying proteins by tandem mass spectrometry. *Anal Chem* **75**: 4646–4658.

Neveu, M., Hays, L.E., Voytek, M.A., New, M.H., and Schulte, M.D. (2018) The ladder of life detection. *Astrobiology* **18**: 1375–1402.

Ni, L., Yang, S., Zhang, R., Jin, Z., Chen, H., Conrad, J.C., and Jin, F. (2016) Bacteria differently deploy type-IV pili on surfaces to adapt to nutrient availability. *NPJ Biofilms Microbiomes* **2**: 1–10.

Nilsson, G., Belasco, J.G., Cohen, S.N., and von Gabain, A. (1984) Growth-rate dependent regulation of mRNA stability in *Escherichia coli*. *Nature* **312**: 75–77.

Noor, E., Bar-Even, A., Flamholz, A., Reznik, E., Liebermeister, W., and Milo, R. (2014) Pathway thermodynamics highlights kinetic obstacles in central metabolism. *PLoS Comput Biol* **10**: e1003483.

Nunn, B.L., Slattery, K.V., Cameron, K.A., Timmins-Schiffman, E., and Junge, K. (2015) Proteomics of *Colwellia psychrerythraea* at subzero temperatures – a life with limited movement, flexible membranes and vital DNA repair. *Environ Microbiol* **17**: 2319–2335.

Oksanen, J., Blanchet, F.G., Kindt, R., Legendre, P., Minchin, P.R., and O'hara, R.B. (2013) Community ecology package. *R package version*, **2**.

Oksanen, J., Guillaume Blanchet, F., Friendly, M., Kindt, R., Legendre, P., McGlinn, D., *et al*. (2019) vegan: community ecology package. R package version 2.5-6. URL https://CRAN.R-project.org/package=vegan.

Oren, A. (2006) *Halophilic Microorganisms and their Environments*. Berlin, Germany: Springer Science & Business Media.

Pahel, G., Rothstein, D.M., and Magasanik, B. (1982) Complex glnA-glnL-glnG operon of *Escherichia coli*. *J Bacteriol* **150**: 202–213.

Parro, V., Blanco, Y., Puente-Sánchez, F., Rivas, L.A., Moreno-Paz, M., Echeverría, A., *et al*. (2016) Biomarkers and metabolic patterns in the sediments of evolving Glacial Lakes as a proxy for planetary Lake exploration. *Astrobiology* **18**: 586–606.

Pawelek, P.D., Croteau, N., Ng-Thow-Hing, C., Khursigara, C. M., Moiseeva, N., Allaire, M., and Coulton, J.W. (2006) Structure of TonB in complex with FhuA, *E coli* outer membrane receptor. *Science* **312**: 1399–1402.

Pema, P.J., Horak, H.A., and Wyatt, R.H. (1998) Myelopathy caused by nitrous oxide toxicity. *Am J Neuroradiol* **19**: 894–896.

Pinto, D., Santos, M.A., and Chambel, L. (2015) Thirty years of viable but nonculturable state research: unsolved molecular mechanisms. *Crit Rev Microbiol* **41**: 61–76.

Pizzarello, S., Cooper, G.W., and Flynn, G.J. (2006) The nature and distribution of the organic material in carbonaceous chondrites and interplanetary dust particles. *Meteorites and the Early Solar System II*. Tuscon, AZ: University of Arizona Press, pp. 625–651.

Pizzarello, S., and Holmes, W. (2009) Nitrogen-containing compounds in two CR2 meteorites: 15N composition, molecular distribution and precursor molecules. *Geochim Cosmochim Acta* **73**: 2150–2162.

Price, P.B. (2000) A habitat for psychrophiles in deep Antarctic ice. *PNAS* **97**: 1247–1251.

Price, P.B., and Sowers, T. (2004) Temperature dependence of metabolic rates for microbial growth, maintenance, and survival. *PNAS* **101**: 4631–4636.

Rabus, R., Ruepp, A., Frickey, T., Rattei, T., Fartmann, B., Stark, M., *et al*. (2004) The genome of *Desulfotalea psychrophila*, a sulfate-reducing bacterium from permanently cold Arctic sediments. *Environ Microbiol* **6**: 887–902.

Rotert, K.R., Toste, A.P., and Steiert, J.G. (1993) Membrane fatty acid analysis of Antarctic bacteria. *FEMS Microbiol Lett* **114**: 253–257.

RStudio Team. (2020) *RStudio: Integrated Development for R*. Boston, MA. URL: RStudio, PBC. http://www.rstudio.com/.

Sageman, B.S., Gardner, M.H., Armentrout, J.M., and Murphy, A.E. (1998) Stratigraphic hierarchy of organic carbon–rich siltstones in deep-water facies, Brushy Canyon Formation (Guadalupian), Delaware Basin, West Texas. *Geology* **26**(5): 451–45.

Sanudo-Wilhelmy, S.A., Cutter, L.S., Durazo, R., Smail, E. A., Gomez-Consarnau, L., Webb, E.A., *et al*. (2012) Multiple B-vitamin depletion in large areas of the coastal ocean. *Proc Natl Acad Sci* **109**: 14041–14045.

Sattler, B., Puxbaum, H., and Psenner, R. (2001) Bacterial growth in supercooled cloud droplets. *Geophys Res Lett* **28**: 239–242.

Shimohata, N., Chiba, S., Saikawa, N., Ito, K., and Akiyama, Y. (2002) The Cpx stress response system of *Escherichia coli* senses plasma membrane proteins and controls HtpX, a membrane protease with a cytosolic active site. *Genes Cells* **7**: 653–662.

Simon, M., and Azam, F. (1989) Protein content and protein synthesis rates of planktonic marine bacteria. *Marine Ecology Progress Series* **51**(3): 201–213.

Showalter, G.M., and Deming, J.W. (2018) Low-temperature chemotaxis, halotaxis and chemohalotaxis by the psychrophilic marine bacterium *Colwellia psychrerythraea* 34H. *Environ Microbiol Rep* **10**: 92–101.

Shultis, D.D., Purdy, M.D., Banchs, C.N., and Wiener, M.C. (2006) Outer membrane active transport: structure of the BtuB:TonB complex. *Science* **312**: 1396–1399.

Skerratt, J.H., Nichols, P.D., Mancuso, C.A., James, S.R., Dobson, S.J., McMeekin, T.A., and Burton, H. (1991) The phospholipid Ester-linked fatty acid composition of members of the family Halomonadaceae and genus Flavobacterium: a chemotaxonomic guide. *Syst Appl Microbiol* **14**: 8–13.

Soutourina, O.A., and Bertin, P.N. (2003) Regulation cascade of flagellar expression in Gram-negative bacteria. *FEMS Microbiol Rev* **27**: 505–523.

Spaans, S.K., Weusthuis, R.A., van der Oost, J., and Kengen, S.W.M. (2015) NADPH-generating systems in bacteria and archaea. *Front Microbiol* **6**(742): 1–27.

Spencer, R.J., Møller, N., and Weare, J.H. (1990) The prediction of mineral solubilities in natural waters: a chemical equilibrium model for the Na-K-Ca-mg-cl-SO4-H2O system at temperatures below 25°C. *Geochim Cosmochim Acta* **54**: 575–590.

Stockton, L., Simonsen, C., and Seago, S. (2017) Nitrous oxide–induced vitamin B12 deficiency. *Proc (Bayl Univ Med Cent)* **30**: 171–172.

Tokunaga, H., Mitsuo, K., Ichinose, S., Omori, A., Ventosa, A., Nakae, T., and Tokunaga, M. (2004) Salt-inducible multidrug efflux pump protein in the moderately Halophilic bacterium *Chromohalobacter* sp. *Appl Environ Microbiol* **70**: 4424–4431.

Torres-Valdés, S., Tsubouchi, T., Davey, E., Yashayaev, I., and Bacon, S. (2016) Relevance of dissolved organic nutrients for the Arctic Ocean nutrient budget. *Geophys Res Lett* **43**: 6418–6426.

Udekwu, K.I., Darfeuille, F., Vogel, J., Reimegård, J., Holmqvist, E., and Wagner, E.G.H. (2005) Hfq-dependent regulation of OmpA synthesis is mediated by an antisense RNA. *Genes Dev* **19**: 2355–2366.

Underwood, G.J.C., Fietz, S., Papadimitriou, S., Thomas, D.N., and Dieckmann, G.S. (2010) Distribution and composition of dissolved extracellular polymeric substances (EPS) in Antarctic Sea ice. *Mar Ecol Prog Ser* **404**: 1–19.

Untersteiner, N., and Sommerfeld, R. (1964) Supercooled water and the bottom topography of floating ice. *J Geophys Res* **69**: 1057–1062.

Vance, S.D., Barge, L.M., Cardoso, S.S.S., and Cartwright, J.H.E. (2019) Self-assembling ice membranes on Europa: Brinicle properties, field examples, and possible energetic systems in icy Ocean Worlds. *Astrobiology* **19**: 685–695.

Ventosa, A., Nieto, J., and Oren, A. (1998) Biology of moderately halophilic aerobic bacteria. *Microbiol Mol Biol Rev* **62**: 504–544.

Vogel, J., and Luisi, B.F. (2011) Hfq and its constellation of RNA. *Nat Rev Microbiol* **9**: 578–589.

Vytvytska, O., Jakobsen, J.S., Balcunaite, G., Andersen, J. S., Baccarini, M., and von Gabain, A. (1998) Host factor I, Hfq, binds to *Escherichia coli* ompA mRNA in a growth rate-dependent fashion and regulates its stability. *Proc Natl Acad Sci U S A* **95**: 14118–14123.

Vytvytska, O., Moll, I., Kaberdin, V.R., von Gabain, A., and Bläsi, U. (2000) Hfq (HF1) stimulates ompA mRNA decay by interfering with ribosome binding. *Genes Dev* **14**: 1109–1118.

Walters, R.F., and DeGrado, W.F. (2006) Helix-packing motifs in membrane proteins. *Proc Natl Acad Sci U S A* **37**: 13658–13663.

Wan, X., Peng, Y.-F., Zhou, X.-R., Gong, Y.-M., Huang, F.-H., and Moncalián, G. (2016) Effect of cerulenin on fatty acid composition and gene expression pattern of DHA-producing strain *Colwellia psychrerythraea* strain 34H. *Microb Cell Fact* **15**: 30.

Wang, H., and Gunsalus, R.P. (2000) The nrfA and nirB nitrite reductase operons in *Escherichia coli* are expressed differently in response to nitrate than to nitrite. *J Bacteriol* **182**: 5813–5822.

Watzer, B., Spät, P., Neumann, N., Koch, M., Sobotka, R., Macek, B., *et al*. (2019) The signal transduction protein PII controls ammonium, nitrate and urea uptake in cyanobacteria. *Front Microbiol* **10**(1428): 1–20.

Wells, L., and Deming, J. (2006b) Characterization of a cold-active bacteriophage on two psychrophilic marine hosts. *Aquat Microb Ecol* **45**: 15–29.

Wells, L.E., and Deming, J.W. (2006a) Modelled and measured dynamics of viruses in Arctic winter sea-ice brines. *Environ Microbiol* **8**: 1115–1121.

Welsh, D.T. (2000) Ecological significance of compatible solute accumulation by micro-organisms: from single cells to global climate. *FEMS Microbiol Rev* **24**: 263–290.

Wickham, H. (2016) *ggplot2: Elegant Graphics for Data Analysis*. New York. URL: Springer-Verlag. https://ggplot2.tidyverse.org.

Wu, G., and Morris, S.M. (1998) Arginine metabolism: nitric oxide and beyond. *Biochem J* **336**: 1–17.

Yun, S.H., Park, E.C., Lee, S.Y., Lee, H., Choi, C.W., Yi, Y. S., *et al*. (2018) Antibiotic treatment modulates protein components of cytotoxic outer membrane vesicles of multidrug-resistant clinical strain, *Acinetobacter baumannii* DU202. *Clin Proteomics* **15**: 28.

Zhang, F., Ouellet, M., Batth, T.S., Adams, P.D., Petzold, C. J., Mukhopadhyay, A., and Keasling, J.D. (2012) Enhancing fatty acid production by the expression of the regulatory transcription factor FadR. *Metab Eng* **14**: 653–660.

Zolotov, M.Y. (2007) An oceanic composition on early and today's Enceladus. *Geophys Res Lett* **34**(L23203): 1–5.

Supporting Information

Additional Supporting Information may be found in the online version of this article at the publisher's web-site:

Table S1. Molal concentrations of sea salt ions used to prepare equilibrium solutions. Concentrations were calculated assuming the equilibrium-freezing pathway of seawater (Marion *et al*., 19991999). Salt concentration (%) was calculated according to Marion and Kargel (20082008). Water activity for brines was calculated based on the equilibrium constant of ice, a function of temperature (Spencer *et al*., 19901990). Note that the equilibrium solution at −1°C corresponds to artificial seawater (ASW).

Table S2. Recipe used in the preparation of experimental saline solutions. Salts (g) added to 1000 g of water.

Table S3. Summary of unique proteins increased in abundance at −5°C compared to controls held at −1°C. All experimental conditions contain samples incubated at −5°C, where Common indicates proteins shared between salinities (ASW or brine). Protein abundance was compared to control to calculate $\log_2$ fold change (LFC), where LFC ≥0.5 indicates significant increase for calculating total number of proteins per condition. Number of unique proteins shows Venn diagram results of proteins uniquely increased in a specific condition or shared salinity. *Calculated as number of proteins identified by EggNOG (Gene Ontology analysis) out of total number proteins significantly changed, indicates percentage of proteins with known classification.

Table S4. Summary of unique proteins decreased in abundance at −5°C compared to controls held at −1°C. All experimental conditions contain samples incubated at −5°C, where Common indicates proteins shared between salinities (ASW or brine). Protein abundance was compared to control to calculate $\log_2$ fold change (LFC), where LFC ≤−0.5 indicates significant decrease for calculating total number of proteins per condition. Number of unique proteins shows Venn diagram results of proteins uniquely decreased in a specific condition or shared salinity. *Calculated as number of proteins identified by EggNOG (Gene Ontology analysis) out of total number proteins significantly changed, indicates percentage of proteins with known classification.

Table S5. Amino acid abundances in the list of enriched k-mers in temperature-specific, salinity-specific conditions of −10°C. Results from chi-squared test to determine which, if any, amino acid compositions of the identified 3-mers and 4-mers were significantly increased or decreased relative to the amino acid distribution of all detected peptide k-mers. Counts are bolded if they are significantly different from the distribution of amino acids in all detected proteins. Additional properties of amino acids are included that are relevant to astrobiology- column L: amino acids that have been observed in most meteorites as reported in Cobb and Pudritz, 19992014, column M: amino acids proposed to be solely the result of metabolic production and have also been detected in CM2 and CR3 meteorites (Pizzarello and Holmes, 20082009) and the rank order of the propensity of that amino acid to be found in an catalytic site in an enzyme where rank order '1' is the most likely, and rank order '20' is least likely to be found in a catalytic site (Bartlett *et al*., 19902002).

Fig. S1. Experimental design for long-term incubations of *Cp*34H in extreme temperatures and salinities. Cells were grown in optimal media at 0°C until desired concentration was reached. Cells were then aliquoted into three separate media with salinity concentrations calculated in Tables 1999S1 and S2. Media for each salinity was divided into two flasks, with or without additional nutrients. Cells were then aliquoted in triplicate to eppendorf tubes and incubated at −5°C or −10°C for 1 and 4 months. Samples were harvested and cell count and culturability measures were performed. Additionally, samples incubated 1 month were measured for activity using [3H]-leu and samples incubated for 4 months were analysed via mass spectroscopy.

Fig. S2. Cell abundance (logarithmic scale) after incubation for 1 and 4 months at −5°C or −10°C. Cell count was performed on cells harvested after incubation for 1 or 4 months.

Open symbols indicate cells incubated in saline solution without nutrients (either ASW: blue, −5°C brine or −10°C brine: orange); filled symbols indicate cells incubated in saline solutions amended with nutrients. Lines connect average values at each time point ($^{+nuts}$: black, $^{-nuts}$: grey). Note that the salinity of equilibrium brines is different for each temperature (see Table 1999S1).

Fig. S3. [3H]-leucine incorporation during early incubation time points. Metabolic activity (3H-leucine incorporation) after incubation first 24 h and 1 month at −5°C or −10°C. Open symbols indicate cells incubated in saline solution without nutrients (either ASW: blue, −5°C brine or −10°C brine: orange); filled symbols indicate cells incubated in saline solutions amended with nutrients. Lines connect average values at each time point ($^{+nuts}$: black, $^{-nuts}$: grey). Dashed line corresponds to the median of controls. Lines connect average values at each time point.

Fig. S4. Proteins quantified and assigned to EggNOG terms. Proteins identified via mass spectrometry to undergo significant changes in abundance compared to optimal conditions (increases shown in red, decreases shown in blue) were mapped to functional orthology enrichment terms using EggNOG. A count was determined (shown in individual boxes) for each experimental condition to identify differences between temperature, salinity and nutrient responses.

Fig. S5. Enriched k-mers attributed to extreme environmental stressor conditions. A) Distribution of k-mers (3–4 amino acid long polypeptides) identified to be enriched in proteins in significantly higher abundances in high salinity (i.e., brine; orange), extreme low temperature (i.e., −10°C; blue) and the combined analysis of high salinity and low temperature (i.e., −10°C brine; purple). Subsets include lists of 3-mers and 4-mers identified to be enriched in more than one condition. B) Heatmap of the distribution of amino acids found in 3-mers (irrespective of position). C) Heatmap of the distribution of amino acids found in 4-mers (irrespective of position). For heatmaps, amino acid counts in each k-mer are represented by rows with no scaling applied, and rows are clustered using Euclidean distance and average linkage. Columns represent treatments and are not clustered (data generated from 1999Dataset S10).

Fig. S6. Nitrogen metabolism in ASW^{+nuts} at −5°C. KEGG pathway map of nitrogen metabolism with proteins detected in ASW^{+nuts} at −5°C as compared to control cells (red: LFC ≥0.5, blue: LFC ≤−0.5, yellow: LFC between 0.5 and −0.5; all: Z-score ≥ 2).

Fig. S7. Arginine biosynthesis in ASW^{+nuts} at −5°C. KEGG pathway map of arginine biosynthesis with proteins detected in ASW^{+nuts} at −5°C as compared to control cells (red: LFC ≥ 0.5, blue: LFC ≤−0.5, yellow: LFC between 0.5 and −0.5; all: Z-score ≥ 2).

Fig. S8. Two-component systems in ASW^{-nuts} at −5°C. KEGG pathway map of two-component systems with proteins detected in ASW^{-nuts} at −5°C as compared to control cells (red: LFC ≥0.5, blue: LFC ≤−0.5, yellow: LFC between 0.5 and −0.5; all: Z-score ≥ 2).

Fig. S9. Ribosomes in brine^{+nuts} at −5°C. KEGG pathway map of individual ribosomal components with proteins detected in brine^{+nuts} at −5°C as compared to control cells (red: LFC ≥0.5, blue: LFC ≤−0.5, yellow: LFC between 0.5 and −0.5; all: Z-score ≥ 2).

Fig. S10. Valine, leucine and isoleucine degradation in brine^{+nuts} at −5°C. KEGG pathway map of branched-chain amino acid degradation with proteins detected in brine^{+nuts} at −5°C as compared to control cells (red: LFC ≥0.5, blue: LFC ≤−0.5, yellow: LFC between 0.5 and −0.5; all: Z-score ≥ 2).

Fig. S11. Fatty acid biosynthesis in brine^{+nuts} at −5°C. KEGG pathway map of fatty acid biosynthesis with proteins detected in brine^{+nuts} at −5°C as compared to control cells (red: LFC ≥0.5, blue: LFC ≤−0.5, yellow: LFC between 0.5 and −0.5; all: Z-score ≥ 2).

Fig. S12. Phenylalanine, tyrosine and tryptophan biosynthesis in brine^{-nuts} at −5°C. KEGG pathway map of phenylalanine, tyrosine and tryptophan biosynthesis with proteins detected in brine^{-nuts} at −5°C as compared to control cells (red: LFC ≥0.5, blue: LFC ≤−0.5, yellow: LFC between 0.5 and −0.5; all: Z-score ≥ 2).

Fig. S13. Carbon metabolism in ASW^{+nuts} at −5°C. KEGG pathway map of carbon metabolism with proteins detected in ASW^{+nuts} at −5°C as compared to control cells (red: LFC ≥0.5, blue: LFC ≤−0.5, yellow: LFC between 0.5 and −0.5; all: Z-score ≥ 2).

Fig. S14. Carbon metabolism in ASW^{-nuts} at −5°C. KEGG pathway map of carbon metabolism with proteins detected in ASW^{-nuts} at −5°C as compared to control cells (red: LFC ≥0.5, blue: LFC ≤−0.5, yellow: LFC between 0.5 and −0.5; all: Z-score ≥ 2).

Fig. S15. Carbon metabolism in brine^{+nuts} at −5°C. KEGG pathway map of carbon metabolism with proteins detected in brine^{+nuts} at −5°C as compared to control cells (red: LFC ≥0.5, blue: LFC ≤−0.5, yellow: LFC between 0.5 and −0.5; all: Z-score ≥ 2).

Fig. S16. Carbon metabolism in brine^{-nuts} at −5°C. KEGG pathway map of carbon metabolism with proteins detected in brine^{-nuts} at −5°C as compared to control cells (red: LFC ≥0.5, blue: LFC ≤−0.5, yellow: LFC between 0.5 and −0.5; all: Z-score ≥ 2).

Dataset S1. Culturability (as MPN), cell counts and activity measurements provided for all samples measured at 1 month.

Dataset S2. Culturability (as MPN) measurements with standard deviations for condition replicates at early experimental time points.

Dataset S3. Calculations and variables used for estimating the number of hours required in each culture, based on the specific conditions and growth rates, to deplete the oxygen within the culture test tube.

Dataset S4. QProt Abacus output generated from all mass spectrometry search results. CSV file that includes normalized spectral abundance factors (NSAF), the number of unique peptides identified for each protein across all experiments, and peptide spectral match (PSM) counts for all confidently identified proteins for each bioreplicate.

Dataset S5. Metadata for NMDS analysis, including nomenclature for temperature, salinity, nutrients, culturability and specific condition labels for each sample.

Dataset S6. Matrix of every protein identified in each condition at −5°C or in the controls at −1°C, where '1' is presence and '0' is absence of the protein as defined by ≥2 unique peptides detected across all experiments, and ≥2 spectral counts per bioreplicate.

Dataset S7. For each protein, normalized NSAF values were calculated for hierarchical clustering analysis as represented by a heatmap, with specific annotations of Uniprot ID and gene name.

Dataset S8. Proteins were assigned a functional annotation of 'Gene.Ontology' using EggNOG-mapper version 5.0, and absolute counts of all proteins passing significance thresholds in each condition were grouped by these functional annotations as increased or decreased.

Dataset S9. Values for UniProt ID, $\log_2$ fold change, z-score, gene ID, gene name, gene ontology as a functional annotation term provided by EggNOG-mapper version 5.0, KEGG number, and original ID are provided for all proteins.

Dataset S10. Excel Workbook with individual lists of enriched k-mers detected in temperature-specific conditions (−10°C), salinity-specific (brine) conditions and −10°C brine conditions (relative to k-mers detected across all treatments. Each Excel tab contains the list of 3- and 4-mers significantly enriched in the specified condition relative to all detected protein k-mers and includes the $\log_2$ fold difference and q-value for each k-mer tested (Brine_specific, Temperature-10_specific, Brine-10_specific). The FullList_k-mers is a complete list of all k-mers identified listed by their conditions and includes the number of occurrences of each amino acid found in each k-mer identified to be increased in abundance in that particular condition and enriched in the condition relative to all detected protein k-mers. The spreadsheet 'k-mer_counts' includes a tabulated list of the number of 3-mers and 4-mers per condition.